

# Journal Pre-proof

Discovery of novel pyrido-pyrrolidine hybrid compounds as alpha-glucosidase inhibitors and alternative agent for control of type 1 diabetes

Tania Luthra, Venkanna Banothu, Uma Adepally, Krishna Kumar, Swathi M, Saikat Chakrabarti, Srinivas R. Maddi, Subhabrata Sen



PII: S0223-5234(20)30001-5

DOI: <https://doi.org/10.1016/j.ejmech.2020.112034>

Reference: EJMECH 112034

To appear in: *European Journal of Medicinal Chemistry*

Received Date: 24 September 2019

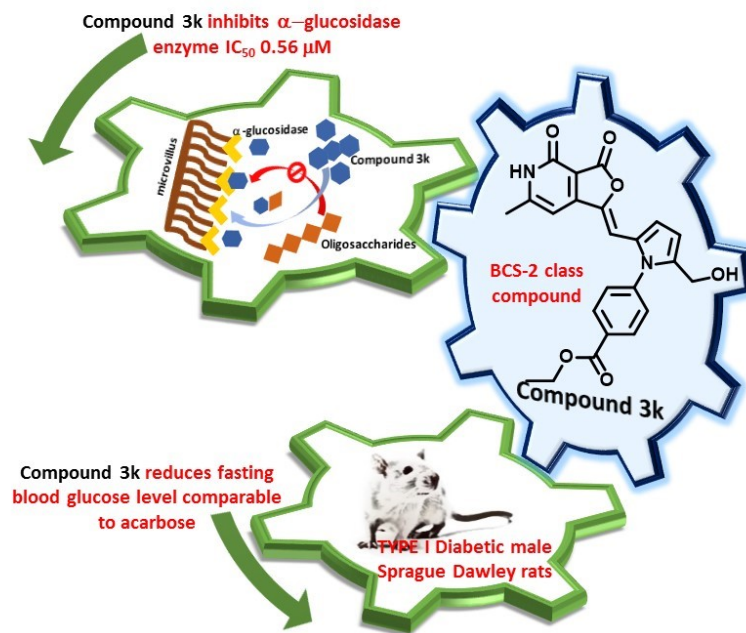
Revised Date: 17 December 2019

Accepted Date: 2 January 2020

Please cite this article as: T. Luthra, V. Banothu, U. Adepally, K. Kumar, S. M, S. Chakrabarti, S.R. Maddi, S. Sen, Discovery of novel pyrido-pyrrolidine hybrid compounds as alpha-glucosidase inhibitors and alternative agent for control of type 1 diabetes, *European Journal of Medicinal Chemistry* (2020), doi: <https://doi.org/10.1016/j.ejmech.2020.112034>.

This is a PDF file of an article that has undergone enhancements after acceptance, such as the addition of a cover page and metadata, and formatting for readability, but it is not yet the definitive version of record. This version will undergo additional copyediting, typesetting and review before it is published in its final form, but we are providing this version to give early visibility of the article. Please note that, during the production process, errors may be discovered which could affect the content, and all legal disclaimers that apply to the journal pertain.

© 2020 Published by Elsevier Masson SAS.



## Discovery of novel pyrido-pyrrolidine hybrid compounds as alpha-glucosidase inhibitors and alternative agent for control of Type 1 diabetes

Tania Luthra,<sup>1</sup> Venkanna Banothu,<sup>2</sup> Uma Adepally,<sup>2</sup> Krishna Kumar,<sup>3</sup> Swathi M,<sup>5</sup> Saikat Chakrabarti,<sup>3</sup> Srinivas R. Maddi<sup>4</sup> and Subhabrata Sen<sup>\*,1</sup>

1. Department of Chemistry, School of Natural Sciences, Shiv Nadar University, Chithera, Dadri, Greater Noida, UP 201314, India
2. Institute of Science and Technology, Jawaharlal Nehru Technological University, Kukatpally, Hyderabad, Telangana 500085, India
3. Structural Biology and Bio-informatics Division, CSIR-Indian Institute of Chemical Biology, 4, Raja SC Mullick Road, Kolkata, West Bengal, 700032, India
4. Acubiosys PVT LTD, TBI, BITS-Pilani Campus, Jawahar Nagar, Hyderabad, Telangana 500078
5. Center for Innovation in Molecular and Pharmaceutical Sciences, Dr. Reddy's Institute of Life Sciences, University of Hyderabad Campus, Gachibowli, Hyderabad-500046

**Keywords:** pyrido-pyrrolidine hybrid; alpha-glucosidase inhibitor; photoluminescence; circular dichroism; DMPK studies

### Abstract

A new library of pyrido-pyrrolidine hybrid compounds were designed, developed and screened for their antidiabetic property with  $\alpha$ -glucosidase. The design is based on preliminary screening of key fragments identified from literature reported  $\alpha$ -glucosidase inhibitors and antidiabetic compounds. The most active fragments were stitched to provide a pyrido-pyrrolidine hybrid molecule as a new motif. A library of these compounds were synthesized and screened against a series of  $\alpha$ -glycosidases. Subsequently, compound **3k** was the most efficacious analog with  $IC_{50}$  of 0.56  $\mu$ M. Photoluminescence study and circular dichroism experiments indicated that compound **3k** modulates the primary and secondary structure of the enzyme. It successfully brings down the fasting blood glucose level for streptozotocin (STZ, 70 mg/kg, Intraperitoneal) induced type I diabetic male Sprague-Dawley rats (250–320 g). At lower concentration, compound **3k** slightly stimulates proliferation of BRIN-BD11 ( $\alpha$ -glucose responsive beta cells from rat pancreas islets that secretes insulin) cells.

### Introduction

Diabetes or diabetes mellitus (DM) is one of the most debilitating non communicable and recurring metabolic disorders in the present world, where nearly 0.5 billion patients are affected globally.<sup>1</sup> It is a condition which occurs due to accumulation of glucose in blood stream leading to hyperglycemia.<sup>2</sup> It is responsible for  $\sim$  5 million deaths every year and it aggravates the rise of heart disease, thrombosis and microvascular complications such as kidney failure, blindness and peripheral

neuropathy.<sup>3</sup> Typically it can be induced either due to the destruction of beta cells *via* autoimmune pathway that results in complete insulin deficiency (type 1 diabetes mellitus [T1DM]) or due to the inability of the body for not using insulin appropriately that leads to resistance towards insulin (type 2 diabetes mellitus [T2DM]).<sup>4</sup> The medical treatment to control the progress of diabetes focuses on reduction of the concentration of postprandial glucose (PG) level in blood.<sup>5</sup>

$\alpha$ -glucosidase enzyme is located at the brush border of intestine, where it is involved in the breakdown of dietary sugars and starches to glucose along with two small intestine membrane bound enzymes maltase-glucoamylase (MGAM) and sucrose-isomaltase (SI). Collectively they are attractive target for inhibition as a way of managing blood glucose levels among individuals suffering from type 2 diabetes.<sup>6</sup> Among them  $\alpha$ -Glucosidase inhibitors (AGI) has been recognized as one of the most important targets for treating T2DM.<sup>6</sup> Few other promising targets include dipeptidyl peptidase 4 (DPP-4), insulin secretagogues, peroxisome proliferator-activated receptor (PPAR- $\gamma$ ) and etc.<sup>7-9</sup> Interestingly, compared to diverse molecular therapy in T2DM, patients suffering from type 1 diabetes (T1DM) insulin is the mainstay for current treatment which, includes maintenance of optimized timing of the pre-meal insulin injection, application of insulin analogues with a faster absorption rate and small molecules that can delay nutrient absorption from the intestine. Several studies have indicated that despite intensive insulin therapy (which involves 3 - 5 insulin injections daily and monitoring of blood glucose level 4 - 5 times a day) nearly 50% of the T1DM affected patients suffer from diabetes related complications such as hypoglycaemia and weight gain.<sup>10-11</sup> Consequently this has prompted the diabetes researchers to look for other potential therapies including  $\alpha$ -glucosidase inhibitors (AGIs) to treat T1DM. Recently few reports indeed indicated that AGIs can also treat insulin deficiency caused by T1DM.<sup>12</sup>

This research aims at developing a novel class of  $\alpha$ -glucosidase inhibitors (AGIs) which can help in controlling high blood glucose level in diabetes mellitus in general. Here in we report discovery of a novel class of molecules based on pyrido-pyrrolidine hybrid for this purpose. The compounds were conceived *via* screening of key fragments of known  $\alpha$ -glucosidase inhibitor and/ or antidiabetic compounds from the literature. They were synthesized in a combinatorial fashion *via* Knoevenagel condensation of pyridofuranone **1** and pyrrolidine based aldehydes **2a - k**. *In vitro* screening against  $\alpha$ -glucosidase enzyme (yeast origin) provided compound **3k** as the most potent inhibitor which displayed competitive inhibition. Fluorescence spectroscopic investigation revealed that compound **3k** modulated the primary structure of  $\alpha$ -glucosidase enzyme. It further attenuates the concentration of  $\beta$ -sheets with the increase in its concentration thereby attuning the secondary

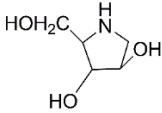
structure. *In vivo* efficacy studies on streptozotocin induced T1DM male Sprague-Dawley rats revealed that compound **3k** reduce concentration of fasting blood glucose level.

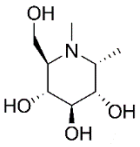
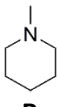
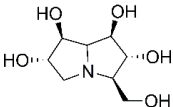
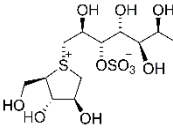
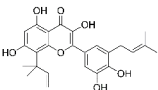
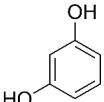
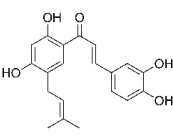
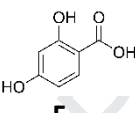
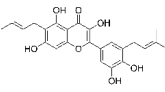
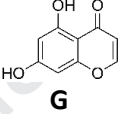
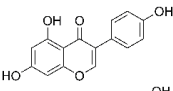
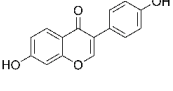
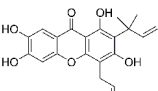
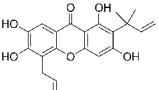
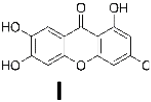
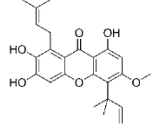
## Results and discussion

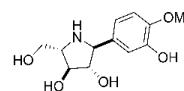
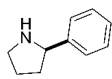
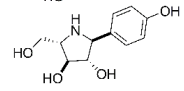
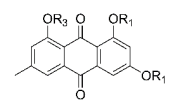
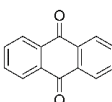
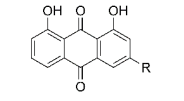
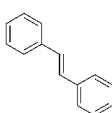
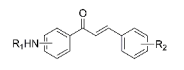
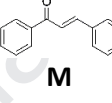
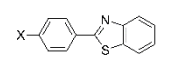
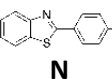
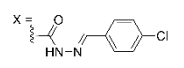
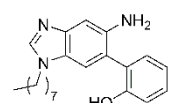
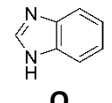
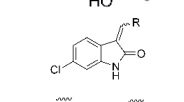
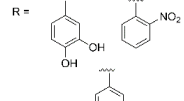
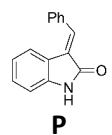
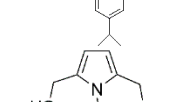
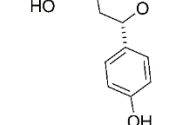
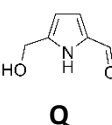
### Design

In order to design novel inhibitors for  $\alpha$ -glucosidase enzyme we manually curated a diverse set of natural and synthetic molecules from the literature which has demonstrated  $\alpha$ -glucosidase inhibition and / or antidiabetic property. These molecules include natural products 4-dideoxy-1, 4-imino-D-arabonitol (DAB), N-methyl- $\alpha$ -homonojirimycin, casuarine, kotalanol, brousochalcone, papyriflavonol A, genistein, dadzein, macluraxanthone, cudraxanthone, cudraticusxanthone F, radicamine A, radicamine B, emodin, physcion, aloe-emodin, rhein, a pyrrole based alkaloid from the fruit peels of *Strychnos nux-blanda*, fumosorinone, and 3-(Z)-butylidenephthalide (Table 1).<sup>13-26</sup> The list also contained synthetic compounds like densely functionalized dibenzyl ether, diaryl- $\alpha$ ,  $\beta$ -unsaturated ketones, benzothiazole and C<sub>3</sub>-alkylidene oxindoles (Table 1).<sup>27-30</sup> The fragments extracted from these molecules comprised of substituted pyrrolidine, piperidines, hexahydropyrrolizine, tetrahydrothiophene, substituted phenols, flavonols, pyranols, anthracenones, anthracene-diones, stilbene, benzothiazole, substituted pyrrolidine, pyridone and pthalide (**A**  $\rightarrow$  **S**). They were either synthesized in-house or procured commercially (Table 1). Screening of these fragments against a series of  $\alpha$ -glycosidases viz. yeast  $\alpha$ -glucosidase,  $\alpha$ -mannosidase (jack bean origin) and  $\alpha$ -mannosidase (bovine kidney origin) resulted in the discovery of three fragments **Q**, **R** and **S**, which were most potent among the fragments screened. Their activity ranged from 5  $\rightarrow$  15  $\mu$ M against  $\alpha$ -glucosidase (yeast origin). This double digit micromolar potency may not look promising however we have to understand these are basic fragments devoid of any functionalities that can augment binding to  $\alpha$ -glucosidase. However these are excellent molecules that could be either functionalized or transformed into more efficacious chemical entities.

**Table 1.** Preliminary fragment screening to search suitable fragments for the design of novel inhibitors against  $\alpha$ -glycosidases (NI; no 50% inhibition at 1 mM concentration of inhibitor)

Compds	Activities as reported in the literature	Fragments	Inhibitory Activity ( $\mu$ M)		
			$\alpha$ -glucosidase (yeast)	$\alpha$ -fucosidase (bovine kidney)	$\alpha$ -mannosidase (jack bean)
	<b>1, 4-dideoxy-1, 4-imino-D-arabonitol (DAB)</b> ; Inhibits yeast $\alpha$ -glucosidase (IC <sub>50</sub> = 0.15 $\mu$ M) and rat intestinal maltase (IC <sub>50</sub> = 5.8 $\mu$ M) <sup>13</sup>	 <b>A</b>	58.01 $\pm$ 1.21	NI	NI

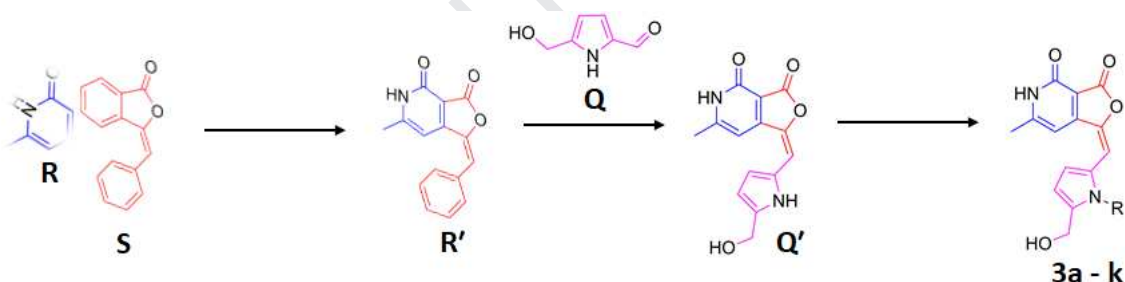
 <p><b>N-methyl-<math>\alpha</math>-homonojirimycin;</b> Inhibits rat intestinal maltase (<math>IC_{50} = 0.72 \mu M</math>) and lowered blood glucose levels in healthy mice<sup>14</sup></p>	 <p><b>B</b></p>	91.88 $\pm$ 0.87	NI	NI
 <p><b>Casuarine</b> Inhibits fungal maltase-glucosidase (<math>IC_{50} = 0.7 \mu M</math>) and rice <math>\alpha</math>-glucosidase (<math>IC_{50} = 1.2 \mu M</math>)<sup>15</sup></p>	 <p><b>C</b></p>	41.12 $\pm$ 2.33	82	51
 <p><b>Kotalanol</b> Inhibits rat intestinal maltase (<math>IC_{50} = 0.18 \mu M</math>)<sup>16</sup></p>	 <p><b>D</b></p>	62.31 $\pm$ 1.02	71	NI
 <p><b>Dimethylallyl-tetrahydroxyflavonol derivative</b> Inhibits <math>\alpha</math>-glucosidase with <math>K_i</math> of 4.2 <math>\mu M</math><sup>17</sup></p>	 <p><b>E</b></p>	NI	NI	NI
 <p><b>Brousochalcone</b> Inhibits <math>\alpha</math>-glucosidase in a non-competitive fashion with <math>K_i = 5.3 \mu M</math><sup>17</sup></p>	 <p><b>F</b></p>	101.22 $\pm$ 3.11	NI	NI
 <p><b>Papyriflavonol A</b> Inhibits <math>\alpha</math>-glucosidase with <math>K_i = 2.3 \mu M</math><sup>17</sup></p>	 <p><b>G</b></p>	85.89 $\pm$ 0.091	89	NI
 <p><b>Genistein</b> Inhibits <math>\alpha</math>-glucosidase with <math>IC_{50} = 7 \mu M</math><sup>38</sup></p>	 <p><b>H</b></p>	81.03 $\pm$ 2.32	54	49
 <p><b>Dadzein</b> Inhibits <math>\alpha</math>-glucosidase with <math>IC_{50} = 14 \mu M</math><sup>18</sup></p>				
 <p><b>Macluraxanthone</b> Inhibits <math>\alpha</math>-glucosidase with <math>K_i = 8.9 \mu M</math><sup>19</sup></p>				
 <p><b>Cudraxanthone</b> Inhibits <math>\alpha</math>-glucosidase with <math>K_i = 7.4 \mu M</math><sup>19</sup></p>	 <p><b>I</b></p>	62.31 $\pm$ 0.41	NI	NI
 <p><b>Cudraticusxanthone F</b> Inhibits <math>\alpha</math>-glucosidase with <math>K_i = 7.0 \mu M</math><sup>19</sup></p>				

	<b>Radicamine A</b> Inhibits $\alpha$ -glucosidase with $IC_{50}$ of $6.7 \mu M$ <sup>20</sup>		$25.21 \pm 1.11$	41	28
	<b>Radicamine B</b> Inhibits $\alpha$ -glucosidase with $IC_{50}$ of $9.3 \mu M$ <sup>20</sup> $R_1 = R_2 = R_3 = H$ ,				
	<b>Emodin</b> , $\alpha$ -glucosidase (yeast), $IC_{50} = 4.12 \mu M$ $R_1 = R_3 = H$ ; $R_2 = Me$ ,				
	<b>Physcion</b> , $\alpha$ -glucosidase (yeast), $IC_{50} = 5.32 \mu M$ $R = CH_2OH$ , <b>Aloe-emodin</b> , $\alpha$ -glucosidase (Yeast), $IC_{50} = 4.56 \mu M$ $R = COOH$ , <b>Rhein</b> , $\alpha$ -glucosidase (Yeast), $IC_{50} = 5.68 \mu M$ <sup>21</sup>		$26.43 \pm 3.39$	32	NI
	Natural product, isolated from <i>Syagmus Romanzoffiana</i> , lowers postprandial blood sugar <i>in vivo</i> <sup>22</sup> a. $R_1 = 3-p$ -tosyl; $R_2 = 4-OH$ and $3, 4$ -di-OH, $\alpha$ -glucosidase (yeast), $IC_{50} = 12$ and $16 \mu M$ b. $R_1 = 4-p$ -tosyl; $R_2 = 4-OH$ or $3, 4$ -di-OH, $\alpha$ -glucosidase (yeast), $IC_{50} = 0.98 \mu M$ and $0.4 \mu M$ <sup>27</sup>		$31.05 \pm 0.71$	NI	NI
			$82.67 \pm 1.54$	91	105
	Benzothiazole with benzohydrazide inhibit $\alpha$ -glucosidase with $IC_{50}$ $5.31$ to $53.3 \mu M$ <sup>28</sup>		$20.54 \pm 0.06$	NI	15
					
	Inhibits yeast $\alpha$ -glucosidase with $IC_{50}$ of $0.16 \mu M$ <sup>29</sup>		$5.03 \pm 1.87$	NI	NI
					
	Inhibits $\alpha$ -glucosidase (yeast) with $IC_{50}$ of $2.71$ , $11.41$ and $14.2 \mu M$ <sup>30</sup>		$15.03 \pm 3.21$	65	28
					
	A pyrrole alkaloid from <i>Strychnos nux-blanda</i> that controls blood sugar <sup>23</sup>		$5.01 \pm 0.66$	21	14

	<b>Fumosorinone (Fu)</b> Inhibits PTP1B activity; increased insulin provoked glucose uptake in insulin resistant HepG2 cells <sup>25</sup>		$14.78 \pm 1.68$	NI	NI
	<b>3-(Z)- butylideneephthalide</b> Reduces blood glucose concn. in NAD-STZ mediaeddiabetic mice. Targets $\alpha$ -glucosidase at the intestinal level and inhibits at $2.15 \mu\text{M}$ non-competitively with $K_i$ $4.86 \mu\text{M}$ . <sup>24</sup>		$7.15 \pm 0.33$	82	41

Data are average of three independent sets of assays performed replicated thrice

In a bid to stitch fragments **Q**, **R** and **S** together to generate new molecules, the aromatic moiety of the pthalide fragment **S**, was replaced with the pyridone fragment **R** to generate the new molecule **R'**. Next the aromatic appendage on **R'** was replaced with the pyrrole moiety **Q** to afford **Q'**. Finally the pyrrole nitrogen on **Q'** was protected with a range of functionalities to provide the desired library (**3a - k**) (Scheme 1).

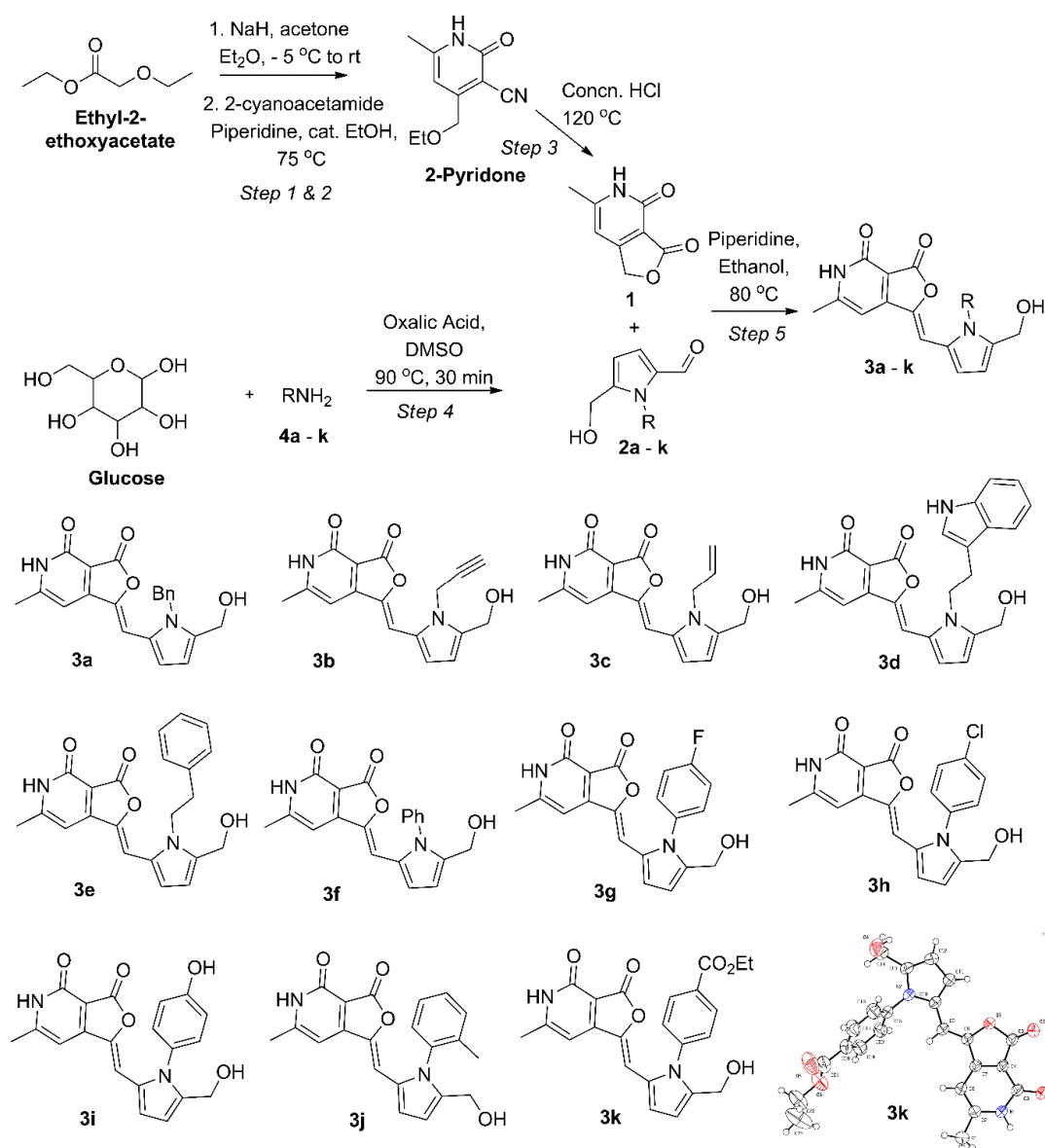


**Scheme 1.** Design of novel  $\alpha$ -glucosidase inhibitors

### Chemistry

The designed compounds were synthesized by Knoevenagel condensation of furopyridine-dione **1** and appropriate pyrrole-2-carbaldehyde derivatives **2a - k**. The synthesis of furopyridine-dione **1** was based on a literature procedure (Step 1 - 3, Scheme 2).<sup>31</sup> To begin with ethyl-2-ethoxyacetate was treated with sodium hydride in presence of acetone to afford ethoxy acetylacetone (Step 1, Scheme 2). It was then treated with 2-cyanoacetamide in piperidine to afford 2-pyridone (Step 2, Scheme 2) which was then lactonized in presence of conc. hydrochloric acid to generate **1** (Step 3, Scheme 2). Pyrrole-2-carbaldehydes **2a - k** were synthesized *via* Malliard reaction in which glucose in presence of oxalic acid was treated with diverse amines **4a - k** (Step 4, Scheme 2).<sup>31</sup> In the final reaction, **1** and **2a - k** were reacted in presence of piperidine which resulted into precipitation of the

desired products (**3a-k**) (Step 5, Scheme 2). They were washed with diethyl ether and hexane to afford the pure compounds **3a - k** (Scheme 2c). The desired compounds were characterized by  $^1\text{H}$  and  $^{13}\text{C}$  NMR analysis and high resolution mass spectroscopy. Single crystal X-Ray of compound **3k** confirmed its structure (Scheme 2) (CCDC# 1934521).



**Scheme 2.** Synthesis of the hybrid library **3a - k**

#### *In vitro* screening against $\alpha$ -glucosidase (yeast origin)

The compound library (**3a - k**) was screened against  $\alpha$ -glucosidase of yeast origin. To assess the extent of selective inhibition of our library molecules they were also screened against  $\alpha$ -fucosidase (bovine liver origin) and  $\alpha$ -mannosidase (jack bean origin). The inhibition was determined in 96-well plates with 4-nitrophenyl- $\alpha$ -D-glucopyranside (PNPG) as the substrate and according to the procedure described in the experimental section. Acarbose was the positive control (Table 2). The

results are tabulated in Table 2. In general, the library is selectively potent against  $\alpha$ -glucosidase compared to  $\alpha$ -fucosidase or  $\alpha$ -mannosidase. Compound **3k** was most potent with an  $IC_{50}$  of 0.56  $\mu$ M which was four times more efficacious than the positive control acarbose ( $IC_{50} = 2.1 \mu$ M). The next potent analogue was compound **3d**, which was moderately active with an  $IC_{50}$  of 4.4  $\mu$ M. It was interesting to see that analogues **3a** and **3f - i** had substantially reduced activity against  $\alpha$ -glucosidase, with  $IC_{50}$  in the range of 20 - 33  $\mu$ M. Compounds **3b, c, e** and **j** demonstrated no activity at all. The structure activity relationship as deduced from this initial screening revealed that pyridine dione as well as the pyrrolidine moiety is important to evoke any inhibitory response against the enzyme. Introduction of a tethered heteroaromatic functionality like a  $C_3$  indolyl moiety to the pyrrolidinyl nitrogen (**3d**) resulted in increased  $\alpha$ -glucosidase inhibitory activity compared to that of a tethered phenyl compound as in compound **3e**. In general aromatic substituents at the pyrrolidinyl nitrogen as exemplified by compound **3f - i**, invoked more potency to the resulting molecules than their aliphatic counterparts **3b** and **c**. Introduction of functionalities on these aromatic rings played a crucial role as epitomized by the *p*-CO<sub>2</sub>Et substituent on the benzene ring in compound **3k**. Interestingly halogens or hydroxy at the *para* position (**compound 3g - i**) or methyl at the ortho substituent (**compound 3j**) of the aromatic moiety had negligible effect on the inhibitory efficacy of the resulting molecules.

**Table 2.** Screening of compounds **3a-k** against various  $\alpha$ -glycosidase (NA: no 50% inhibition at 1 mM concentration of the compound)

Compounds	$IC_{50}$ in $\mu$ g/ mL		
	$\alpha$ -glucosidase (yeast origin)	$\alpha$ -fucosidase (bovine kidney origin)	$\alpha$ -mannosidase (jack bean origin)
<b>3a</b>	20.8 $\pm$ 0.65	51.1 $\pm$ 1.21	92.3 $\pm$ 2.43
<b>3b</b>	NA	NA	NA
<b>3c</b>	NA	NA	NA
<b>3d</b>	4.4 $\pm$ 1.09	12.9 $\pm$ 1.11	NA
<b>3e</b>	NA	NA	NA
<b>3f</b>	27.4 $\pm$ 0.72	38.4 $\pm$ 1.28	61.4 $\pm$ 2.38
<b>3g</b>	20.7 $\pm$ 0.77	NA	NA
<b>3h</b>	21.9 $\pm$ 1.34	NA	NA
<b>3i</b>	33.3 $\pm$ 2.11	21.7 $\pm$ 1.14	NA
<b>3j</b>	NA	NA	NA
<b>3k</b>	0.56 $\pm$ 0.11	30.4 $\pm$ 0.69	41.2 $\pm$ 0.82

<b>Acarbose</b>	$2.1 \pm 0.78$		
-----------------	----------------	--	--

Data are average of three sets of assays performed

### Reaction kinetics

To evaluate the mechanism of binding of the most active inhibitor **3k** with  $\alpha$ -glucosidase (yeast origin), kinetics analysis was performed. The type of inhibition and  $K_i$  were obtained from the Lineweaver-Burke plots as shown in figure 1. The experiments were conducted at 37 °C. The  $K_i$  was obtained from  $V_{max}$  at 2  $\mu$ M and 10  $\mu$ M of compound **3k**. The experiments showed that compound **3k** was a competitive inhibitor with  $K_i$  value of 29.91  $\mu$ M. The kinetic analysis further suggested that compound **3k** competes with substrate for binding at active site of the  $\alpha$ -glucosidase enzyme (yeast origin) (Figure 1a). Figure 1b depicts a linear Lineweaver-Burk plot for the standard drug acarbose.

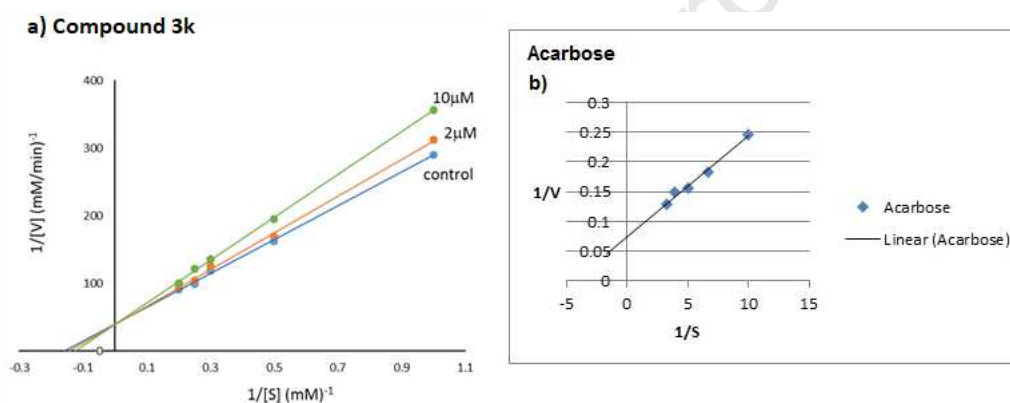


**Figure 1.** a) Reactions kinetics experiments to assess the mechanism of action of compound **3k** on the  $\alpha$ -glucosidase enzyme (yeast origin). b) Reaction kinetics study of acarbose

### Investigation of interaction between $\alpha$ -glucosidase enzyme (yeast origin) and compound 3k with Fluorescence spectroscopy

Fluorescence spectroscopic investigation of ligand-protein complex determines the alteration of protein conformation along with binding mechanism (static or dynamic), binding sites and binding constants. The tryptophan (Trp) residue of  $\alpha$ -glucosidase enzyme emit fluorescence upon activation and hence fluorescence spectroscopy can be harnessed to assess the extent of modulation of  $\alpha$ -glucosidase conformation imposed by an inhibitor.<sup>32</sup> In general the resulting fluorescence emission of an inhibitor bound  $\alpha$ -glucosidase enzyme will decrease compared to the free enzyme. This phenomenon is known as fluorescence quenching. With the steady increment of the concentration of the inhibitor the fluorescence intensity is further quenched, thereby indicating the extent to which the ligand binds to the enzyme. Accordingly the fluorescence quenching experiment of compound **3k** with  $\alpha$ -glucosidase enzyme (yeast origin) was conducted and the result is depicted in

figure 2. Excitation of  $\alpha$ -glucosidase (yeast origin) at a wavelength of 295 nm, displayed a strong fluorescence emission peak at 330 nm. Inherently compound **3k**, had no fluorescence emission and contributed negligibly to the fluorescence interference. Next, addition of inhibitor **3k** at 6.25 ng/mL and 25 ng/mL led to the decrease of intrinsic fluorescence spectra of  $\alpha$ -glucosidase significantly at 298 K (Figure 2). This indicated that compound **3k** binds to  $\alpha$ -glucosidase, and the binding could be induced through a microenvironment variation of Trp residues in  $\alpha$ -glucosidase enzyme.

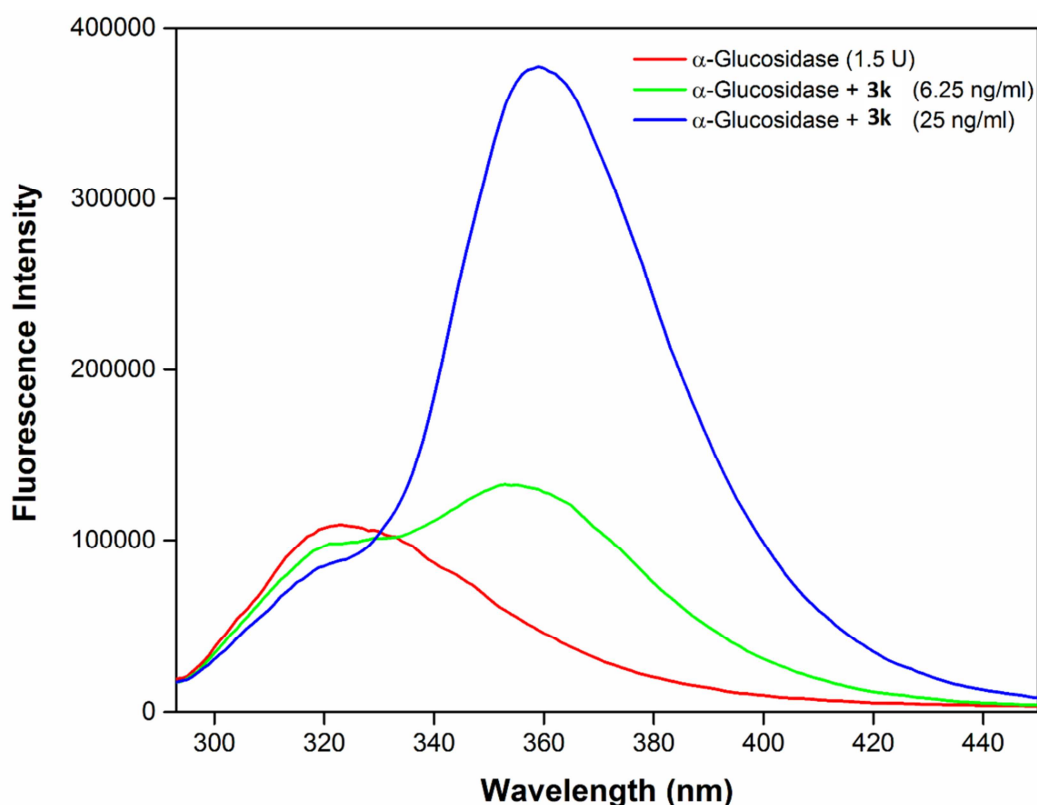
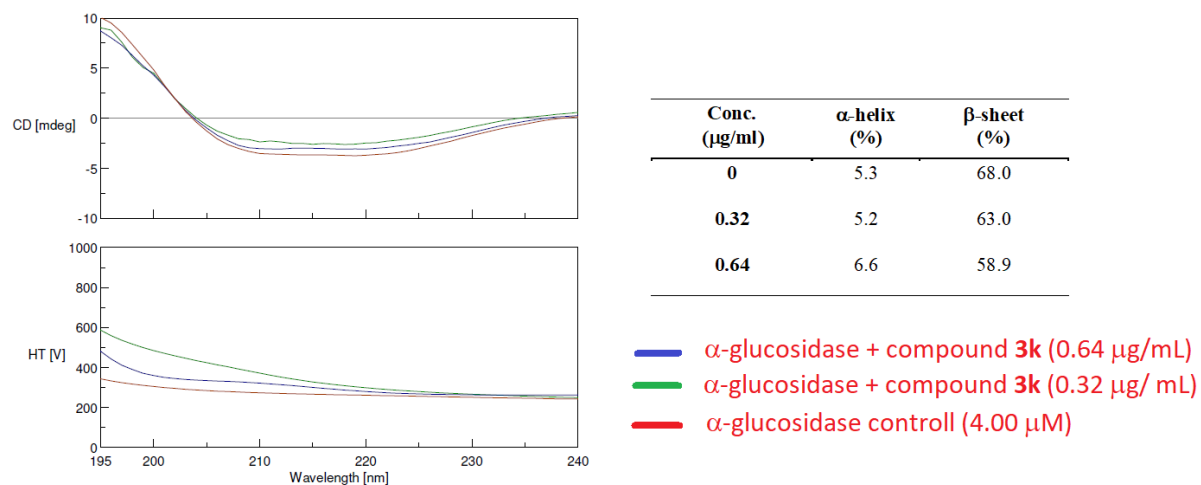


Figure 2. Fluorescence quenching spectra of compound **3k**

#### ***Investigation of modulation of 2<sup>o</sup> structure of $\alpha$ -glucosidase enzyme (yeast origin) by **3k*****

Circular dichroism (CD) is a technique that can be used to understand the conformational changes of a protein when modulated by a ligands. Herein, we utilized CD to assess the alteration in secondary structure of  $\alpha$ -glucosidase induced by compound **3k** (Figure 3).<sup>33</sup> The CD spectrum of  $\alpha$ -glucosidase (Figure 3) included 2 negatively humped peaks at 209 and 222 nm which further revealed that  $\alpha$ -glucosidase has a high percentage of  $\alpha$ -helical structures.<sup>34</sup> In the presence of compound **3k**, the intensity of these peaks were reduced when compared to the control (Figure 3). This implied that the helicity of  $\alpha$ -glucosidase was decreased once it interacts with compound **3k**. The Secondary Structure Estimation Program calculated the secondary structural content of  $\alpha$ -glucosidase. It was observed that as the concentration of compound **3k** increased, the percentages of  $\beta$ -sheets in  $\alpha$ -glucosidase got decreased, (Figure 3). Hence, the binding of compound **3k** to  $\alpha$ -glucosidase induced

alterations in the secondary structure of  $\alpha$ -glucosidase and modulated the folding of the protein. This probably contributed to the inhibition pathway whereby compound **3k** prevented substrate binding that lead to the inhibition of  $\alpha$ -glucosidase (Figure 3).



**Figure 3.** Circular Dichroism spectra of compound **3k** with  $\alpha$ -glucosidase (yeast origin)

#### ***Molecular modelling of compound 3k against a homology model of 3D structure of alpha-glucosidase from Saccharomyces cerevisiae***

The 3D structure of alpha-glucosidase from *Saccharomyces cerevisiae* was generated using homology modelling approach and further *in-silico* validation of the model structure was performed (see Methods). The compound **3k** was docked by the GOLD program onto the CASTp predicted binding pocket (Figure 4, panel B) of alpha-glucosidase and most plausible solution was identified based on the CHEMPLP score (69.87) of the GOLD suite. The estimated  $\Delta G$  of binding was found to be -15.53. The selected protein - compound **3k** complex was further investigated for the interaction analysis. Accordingly probable interacting residues were identified. Four probable hydrogen bonds were observed to be formed between protein and compound **3k** (Figure 4, panel D).

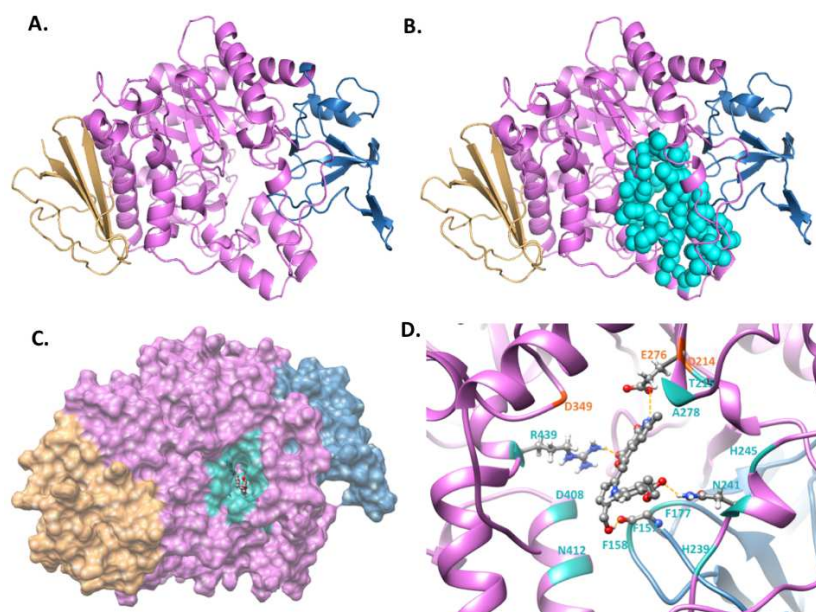


**Figure 4.  $\alpha$ -Glucosidase modelling and docking.** (A) 3D model structure of  $\alpha$ -glucosidase (yeast) (MAL32) protein (PDB ID: 3AJ7) is shown in cartoon representation where domain A (residues: 1-112 and 189-509), domain B (residues: 113-188), and domain C (residues: 510-584) are marked in gold, pink and blue colors, respectively. (B) Largest ligand binding pocket identified by CASTp is marked by cyan spheres. (C) GOLD predicted most likely complex of compound **3k** and yeast alpha-glucosidase (MAL32) protein is shown in surface representation where binding pocket is shown in cyan. (D) Protein-compound **3k** interacting residues are shown in cyan and previously reported catalytic residues D214, E276 and D349 are shown in orange. Probable hydrogen bonds are indicated by yellow dotted lines.<sup>35-38</sup>

#### **DMPK studies**

Drug metabolism and pharmacokinetics is essential within drug discovery and development. It provides information about absorption, metabolism and excretion (ADME) processes of a drug molecule in a physiological system.<sup>39</sup> This information contributes to better designing of drugs and avoidance of drug-drug interaction (DDI). The primary role of DMPK studies is to subscribe the optimisation of the compounds for *in vivo* experiments by considering various physicochemical properties gathered from *in vitro* experiments with materials obtained from human beings and *in vivo* animal studies.<sup>39</sup> Accordingly thermodynamic solubility, log D and PAMPA permeability of compound **3k** was determined. The metabolic stability of compound **3k** in mouse, rat and human liver microsomes were measured. Its ability to bind to plasma in mouse, rat and human plasma were also measured. Finally pharmacokinetics of compound **3k** in mice was investigated.

The physicochemical characterization studies of compound **3k** demonstrated that it is a poorly soluble (solubility  $\sim 0.1$  mg/ mL in phosphate buffer at pH 7.4) and highly permeable compound as understood from the GIT PAMPA data in table 3. This categorizes it to BCS-2 class of compounds.

**Table 3.** Thermodynamic solubility data of compound **3k** at 1mg/mL in phosphate buffer at pH 7.4

Solubility (ug/mL)	Log D	GIT PAMPA at pH 7.4	$P(10^{-6}\text{cm/s})$
0.1	2.4		15

The high metabolic clearance of compound **3k** in human, rat and mouse microsomes as shown in Table 4 indicated rapid degradation of this compound in liver. The clearance is mainly due to CYP mediated phase-1 metabolism.

**Table 4:** Metabolic stability data of compound **3k** in liver microsomes of mouse, rat and human

Species	Percent metabolized	$t_{1/2}$ (min)	mCLint (uL/min/kg)	CL <sub>in vivo</sub> (mL/min/kg)
Mouse	99.03 $\pm$ 0.01	9	74.11 $\pm$ 2.03	60.31 $\pm$ 0.11
Rat	95.21 $\pm$ 0.33	15	54.41 $\pm$ 0.09	35.22 $\pm$ 1.54
Human	96.33 $\pm$ 1.22	13	54.78 $\pm$ 1.21	15.09 $\pm$ 0.91

The variation in the plasma protein binding from human, mouse and rat may be due to low recovery of the compound **3k** which was explained by its nonspecific binding to the plasma protein (Table 3).

**Table 5.** Plasma protein binding data of compound **3k** at 10  $\mu$ M in liver microsomes of mouse, rat and human

Species	Percent free fraction	Percent bound fraction	% recovery
Mouse	8.99 $\pm$ 0.20	91.01 $\pm$ 0.21	15.02 $\pm$ 0.47
Rat	1.56 $\pm$ 0.32	98.44 $\pm$ 0.32	1.95 $\pm$ 0.40
Human	10.74 $\pm$ 2.10	89.26 $\pm$ 2.10	56.66 $\pm$ 4.90

Following PO administration in swiss albino mouse, compound **3k** demonstrated low oral exposure (Figure 5), which could be due to its poor solubility in the intestine which was also evidenced by low thermodynamic solubility.

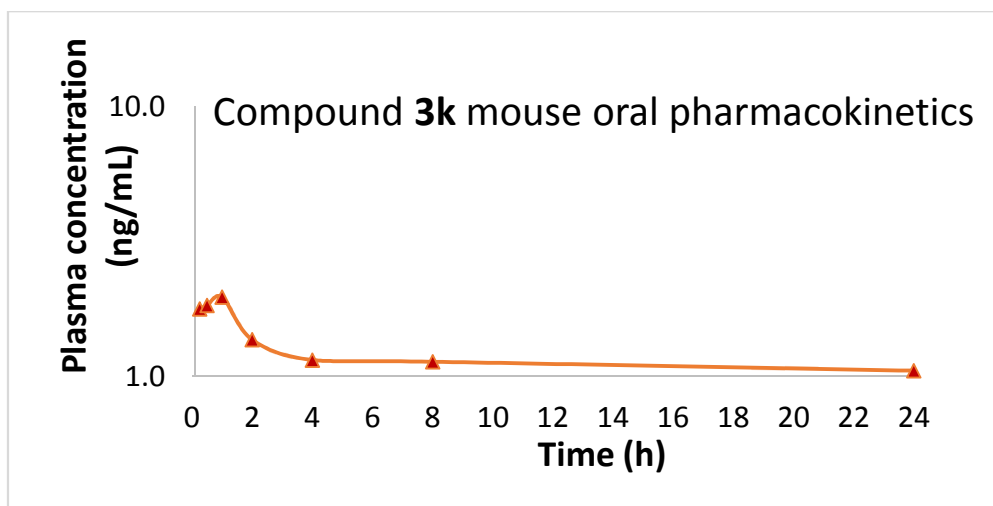


**Figure 5.** Pharmacokinetics of compound **3k** after oral administration into male Swiss albino mice at 3mg/kg

The solubility (Kinetic and thermodynamic) and permeability (PAMPA) studies of compound **3k** indicated that it was a poor soluble and high permeable compound which resembles to BCS class II category. The stability of compound **3k** in human, rat and mouse microsomes demonstrated that it was unstable and revealed high metabolic clearance, indicating that the clearance was mainly due to CYP mediated phase -1 metabolism. The variation in protein binding of compound **3k** from human, mouse and rat plasma may be due to low recovery of the compound, which could be due to poor solubility and nonspecific binding of the compound. Investigations are underway to understand the rapid metabolism of compound **3k** and to identify the soft spot responsible for degradation.

#### ***In vivo* efficacy**

Male Sprague Dawley rats (250 - 320g) were utilized in *in vivo* studies. Diabetes was induced through administration of a single dose of Streptozotocin (STZ, 70 mg/kg, intraperitoneal) formulated in 0.1 mmol/L citrate buffer, pH 4.5 (Sigma-Aldrich, India). Random blood glucose above 125 mg/dl was used to consider rats as diabetic. This blood glucose level were compared with normal vehicle control animals (n=6). Diabetic rats were provided a normal diet throughout the experiment. Diabetic rats (with similar degree of hyperglycaemia) were divided arbitrarily into three groups and were assigned as diabetic vehicle, diabetic acarbose (the group treated with acarbose (used as -ve control), and diabetic **3k** (the third group treated with compound **3k**) (n = 6, in each group).

The fasting blood glucose values of diabetic rats were significantly higher than those of control rats at week zero ( $P < 0.001$ ), week one ( $P < 0.0001$ ), week two ( $P < 0.0001$ ), week three ( $P < 0.0001$ ) and week four ( $P < 0.0001$ ) (Figure 6). The same in the diabetic acarbose decreased significantly at week one ( $P < 0.0001$ ), week two ( $P < 0.0001$ ), week three ( $P < 0.0001$ ), and week four ( $P < 0.0001$ ) compared to the diabetic vehicle. Interestingly fasting blood glucose values in the group diabetic **3k** decreased

significantly at week one ( $P<0.0001$ ) and week two ( $P<0.0001$ ), but displayed values above the diabetic acarbose group at week three ( $P<0.0001$ ), and week four ( $P<0.0001$ ) in comparison to the diabetic group (Figure 6a).

It is noteworthy that both acarbose and compound **3k**, were unable to bring down the non-fasting (postprandial) blood glucose level during the entire four weeks of investigation, when compared with the diabetic group (Figure 6b). For acarbose this inability can be explained, as it works only in TYPE 2 diabetes mellitus, but this efficacy study was against TYPE 1 diabetes mellitus model (Streptozotocin induced). Interestingly the mean body weight of diabetic rats significantly reduced compared to control rats. No significant results were noted between diabetic group and acarbose/compound **3k** treated groups (Figure 6c).

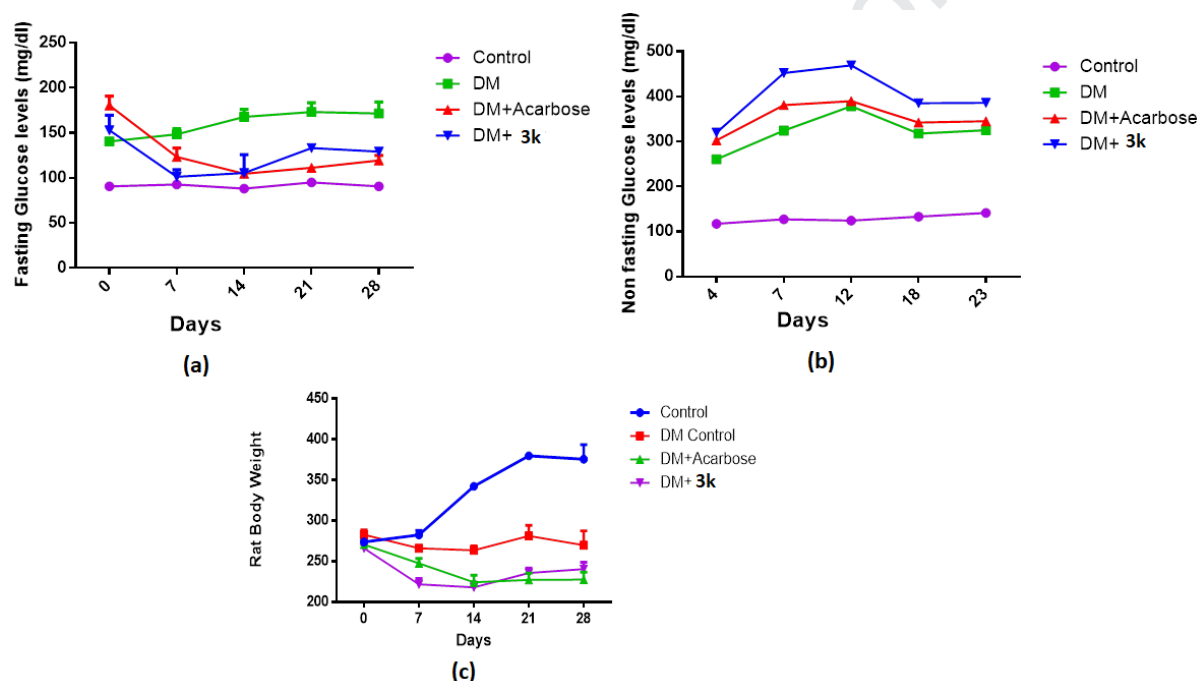


**Figure 6.** (a) Fasting blood glucose before and after acarbose and compound **3k** treatment in male rats ( $n = 6$  per group) ( $***P<0.0001$  versus the control group;  $***P<0.0001$  versus the DM group [DM = Diabetes Mellites]; Data represents mean  $\pm$  SD ( $n=6$ )). (b) Non-fasting blood glucose prior and later acarbose and compound **3k** treatment in male rats ( $***P<0.0001$  Vs the control group;  $***P<0.0001$  versus the DM group; Data represents mean  $\pm$  SD ( $n=6$ )). (c) Body weight before and after acarbose and compound **3k** treatment in rats (Statistical analysis results are expressed as the mean  $\pm$  standard deviation. Statistical analysis was performed with 2-way ANOVA.  $P<0.0001$  was considered statistically significant. Analysis performed with Graph prism 6.01). Note. There is a minute statistical difference, hence the error bars not clearly visible in this graph.

### $\beta$ -cell proliferation study

$\beta$ -cells are found in pancreatic islets and are known to enact a crucial role in metabolism by modulating glucose homeostasis through the production of insulin. A current prognoses in type 1 diabetes mellitus (T1DM) based on genetic and environmental implication indicates selective targeting of  $\beta$ -cells by the immune system that leads to the loss of functional  $\beta$ -cell mass.<sup>40-41</sup> Hence one of the promising therapies for T1D is envisioned as development of small molecules that can address  $\beta$ -cell dysfunction by promoting regeneration of  $\beta$ -cell mass. Since the *in vivo* investigation of compound **3k** against T1DM induced S/D rats demonstrated reduction of fasting blood glucose values, it was further subjected to  $\beta$ -cell proliferation studies. Accordingly MTT assay against BRIN-BD11 cells (rat beta cell line) was conducted with compound **3k** (refer experimental). Cells were exposed to compound **3k** at varying concentration *viz.* 100, 30, 10, 3, 1, 0.3 and 0.1  $\mu$ M in 100  $\mu$ L medium. Interestingly compound **3k** exhibited marginal proliferation of the b-cells at low concentration ( $\rightarrow$  1  $\mu$ M) (Figure 8) but exerted minimum cytotoxic effect at higher concentration ( $\geq$  10  $\mu$ M). However the minor cytotoxic effect remained unchanged with further increase in the concentration of compound **3k** (Figure 7).

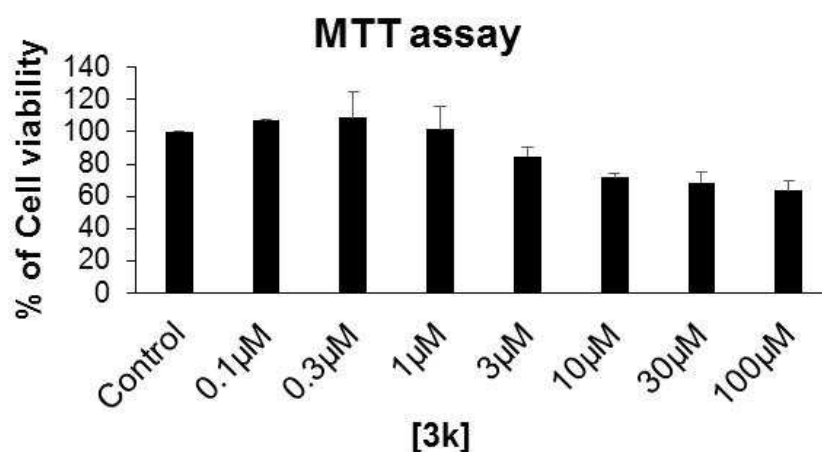


**Figure 7.** Compound **3k** induces b-cell proliferation in BRIN-BD11 cells (rat beta cell line)

## Discussion

Herein we have reported discovery of a novel series of pyrido-pyrrolidine hybrid compounds as  $\alpha$ -glucosidase inhibitors. Preliminary screening of the fragments of known  $\alpha$ -glucosidase inhibitors and antidiabetic compounds provided the key moieties, which were merged to generate the new molecules. The compounds were synthesized *via* Knoevenagel condensation of appropriate substrates **1** and **2** to provide the compounds. Next the compounds were screened against  $\alpha$ -glucosidase of yeast origin. When compared to human  $\alpha$ -glucosidase, they shared similarity in substrate specificity, pH optimum and towards inhibitor sensitivity. Additionally, modification of the arginine, tryptophan and cysteine residue of both the enzymes render them inactive. The initial

assay indicated that compound **3k** is the most active compound with  $IC_{50} \sim 0.56 \mu\text{M}$ . It is four times as potent as the standard drug acarbose ( $IC_{50} \sim 2 \mu\text{M}$ ). Photoluminescence and CD study demonstrated that compound **3k** modulate primary and secondary structure of the enzyme. From the reaction kinetics study it was further revealed that **3k** is a competitive inhibitor. DMPK experiments demonstrated that due to poor solubility and high permeability compound **3k** belongs to BCS-2 class of compounds, where its exposure is low when administered orally.  $\alpha$ -glucosidase inhibitors are generally used to remit the blood glucose concentration of patients suffering from T2DM. Recently they were successfully applied to patients suffering from T1DM. This encouraged us to assess the efficacy of compound **3k** against S-D rats induced with T1DM by streptozotocin. Accordingly we observed that compound **3k** when administered against S-D rats was unable to bring down the non-fasting (postprandial) blood glucose level during the entire four weeks of investigation. This was almost comparable with acarbose (standard drug). However, compound **3k** was able to reduce the fasting blood glucose values of diabetic rats which was almost same as compared with acarbose. Hence *in vitro* ADME and *in vivo* efficacy studies of **3k** indicated that the solubility of the compounds need to be increased and permeability needs to be brought down. Probably the acid analogue of **3k** could improve the solubility and appropriate protection of its hydroxy moiety could provide the appropriate permeability. Research is presently ongoing in our lab in this direction. Investigation with  $\beta$ -cells revealed that compound **3k** induces slight stimulation of the proliferation of  $\beta$ -cells at lower concentration, however at higher concentration there was not much cytotoxicity observed. This is not unexpected as **3k** functioned through inhibition of  $\alpha$ -glucosidase to bring down the blood glucose level. The uniqueness of this investigation is,  $\alpha$ -glucosidase inhibitors (which are typically meant for controlling T2DM) demonstrated reduction of blood glucose level in T1DM induced S-D rats. To further understand the dose dependent efficacy of **3k**, we have planned to dose with multiple doses in type 1 and type 2 diabetes models as a future study. We sincerely hope this investigation provides a robust platform to advance such chemotypes as small molecule therapeutics against T1DM.

### Conclusion

In conclusion, a new pyrrolo pyridone hybrid molecule was identified as an  $\alpha$ -glucosidase inhibitor through fragment screening of known  $\alpha$ -glucosidase inhibitor. It showed strong and selective inhibitory activity against yeast  $\alpha$ -glucosidase. It presented potent competitive inhibition against the enzyme. Preliminary structure activity relationship (SAR) studies suggested the existence of pyridine dione and the pyrrole moiety to play crucial role in the inhibitory activity against  $\alpha$ -glucosidase.

**3k**, the most potent inhibitor was further evaluated for its *in vitro* ADME and *in vivo* efficacy. It demonstrated efficacious hypoglycemic reaction in streptozotocin induced S-D rats (fasting blood

glucose). However poor solubility, high permeability and low oral exposure of **3k**, renders room for improvement in ADME features of this molecule. However on the basis of these initial investigation we anticipate **3k** could be a potential hit compound for new drug discovery.

### Experimental

*Chemistry:* All reactions were carried out in flame-dried sealed tubes with magnetic stirring. All experiments were performed under argon atmosphere. All reagents were purchased from Sigma Aldrich or Alfa Aesar. Reaction was monitored by thin layer chromatography (TLC, Silica gel 60 F254), using UV light to visualize the course of the reaction.  $^1\text{H}$  NMR and  $^{13}\text{C}$  NMR spectra were recorded with tetramethylsilane as an internal standard at ambient temperature unless otherwise indicated with Bruker 400 MHz instruments at 400 MHz for  $^1\text{H}$  NMR and 100 MHz for  $^{13}\text{C}$  NMR spectroscopy. Splitting patterns are designated as singlet (s), broad singlet (br, s), doublet (d), triplet (t). Splitting patterns that could not be interpreted or easily visualized are designated as multiplet (m). Mass spectrometry analysis was done with a 6540 UHD Accurate-Mass QTOF LC- MS system (Agilent Technologies) equipped with an Agilent 1290 LC system obtained by the Department of Chemistry, School of Natural Sciences, Shiv Nadar University, Uttar Pradesh 201314, India. HPLC analysis was conducted using Gradient pump mode with A (ACN) and B (0.1% formic acid in water) as eluent for 10 minutes. The retention time (tR) is expressed in min at UV detection of 254 nm. HPLC analysis was performed on an Agilent Eclipse Plus C18 (4.6 × 50 mm, 3.5  $\mu\text{m}$ ) at 30 °C. Flow rate: 0.5 mL/min.

Compounds **2a-k** were synthesized from a standard protocol reported in the literature.<sup>13</sup>

*General Procedure for synthesis of compound 3a-k.* To the stirred solution of 6-methylfuro[3,4-c]pyridine-3,4(1H,5H)-dione (200 mg, mmole) (1 equivalence) in ethanol (10 ml), piperidine (1 equivalence) was added. To the stirring solution appropriate pyrrole **2a-k** (1 equivalence) were added under nitrogen atmosphere and the resulting reaction mixture was refluxed at 80°C for 14 hours within which substantial amount of product precipitates from the reaction mixture. Then reaction mixture was cooled to room temperature and was filtered and the solid obtained was washed with diethyl ether and hexane respectively (2 X 5 mL) and desired product was dried.

#### **(Z)-1-((1-benzyl-5-(hydroxymethyl)-1H-pyrrol-2-yl)methylene)-6-methylfuro[3,4-c]pyridine-3,4(1H,5H)-dione (3a)**

Following the general procedure, the desired compound **3a** was synthesized from (furopyridindione (200mg, 1.21 mmol), 1-benzyl-5-(hydroxymethyl)-1H-pyrrole-2-carbaldehyde (260mg, 1.21 mmol) and piperidine (0.12 ml, 1.21 mmol). A brown solid was generated with yield of 75%.

$^1\text{H}$  NMR (400 MHz; DMSO- $d_6$ ):  $\delta$  2.62 (s, 3H); 4.37 (s, 2H); 5.51(s, 2H); 6.33-6.32 (d,  $J$  = 3.92 Hz, 1H); 6.66 (s, 1H); 6.90 (s, 1H); 6.95-6.94 (d,  $J$  = 3.88 Hz, 1H); 6.99-6.97 (d,  $J$  = 7.40 Hz, 2H); 7.24-7.20 (m,

1H); 7.32-7.27 (m, 2H).  $^{13}\text{C}$  NMR (100 MHz; DMSO- $d_6$ ):  $\delta$  19.48, 39.52, 46.08, 55.36, 96.37, 101.71, 104.31, 111.09, 115.66, 125.88, 127.11, 127.17, 128.63, 138.46, 138.56, 138.77, 154.07, 155.38, 157.93, 164.20. IR (neat,  $\nu$   $\text{cm}^{-1}$ ): 3459, 2920, 1782, 1666, 1610, 1280.  $[\text{M}+\text{H}]^+$  calculated for ( $\text{C}_{21}\text{H}_{18}\text{N}_2\text{O}_4$ ) 363.139 found 363.1447. Melting point: 265  $^\circ\text{C}$ .

**(Z)-1-((5-(hydroxymethyl)-1-(prop-2-yn-1-yl)-1H-pyrrol-2-yl)methylene)-6-methylfuro[3,4-c]pyridine-3,4(1H,5H)-dione (3b)**

Following the general procedure, the desired compound **3b** was synthesized from (furopyridindione (200mg, 1.21 mmol), 5-(hydroxymethyl)-1-(prop-2-yn-1-yl)-1H-pyrrole-2-carbaldehyde (197mg, 1.21 mmol) and piperidine (0.12 ml, 1.21 mmol). A brown solid was generated with yield of 78%.

$^1\text{H}$  NMR (400 MHz; DMSO- $d_6$ ):  $\delta$  2.31 (s, 3H); 3.37 (s, 1H); 4.53 (s, 2H); 5.10 (s, 2H); 6.25-6.24 (d,  $J$  = 3.76 Hz, 1H); 6.77 (s, 1H); 6.85-6.84 (d,  $J$  = 3.84 Hz, 1H); 6.99 (s, 1H).  $^{13}\text{C}$  NMR (100 MHz; DMSO- $d_6$ ):  $\delta$  19.98, 33.12, 55.57, 75.81, 80.05, 96.92, 101.80, 104.88, 111.40, 116.12, 127.10, 138.28, 139.40, 154.73, 155.93, 158.41, 164.67. IR (neat,  $\nu$   $\text{cm}^{-1}$ ): 3240, 2917, 2110, 1767, 1661, 1612, 1227, 639.  $[\text{M}+\text{H}]^+$  calculated for ( $\text{C}_{17}\text{H}_{14}\text{N}_2\text{O}_4$ ) 311.1026 found 311.1019. Melting point: 276  $^\circ\text{C}$

**(Z)-1-((1-allyl-5-(hydroxymethyl)-1H-pyrrol-2-yl)methylene)-6-methylfuro[3,4-c]pyridine-3,4(1H,5H)-dione (3c)**

Following the general procedure, the desired compound **3c** was synthesized from (furopyridindione (200mg, 1.21 mmol), 1-allyl-5-(hydroxymethyl)-1H-pyrrole-2-carbaldehyde (200mg, 1.21 mmol) and piperidine (0.12 ml, 1.21 mmol). A orange solid was generated with yield of 80%.

$^1\text{H}$  NMR (400 MHz; DMSO- $d_6$ ):  $\delta$  2.30 (s, 3H); 4.43 (s, 2H); 4.80-4.76 (m, 1H); 4.87 (s, 2H); 5.09-5.07 (d,  $J$  = 10.32 Hz, 1H); 5.18 (s, 1H); 5.97-5.96 (m, 1H); 6.26-6.25 (d,  $J$  = 3.88 Hz, 1H); 6.82-6.76 (m, 2H); 6.87-6.86 (d,  $J$  = 3.84 Hz, 1H); 11.86 (s, 1H).  $^{13}\text{C}$  NMR (100 MHz; DMSO- $d_6$ ):  $\delta$  19.95, 45.69, 55.64, 96.88, 102.25, 104.74, 111.16, 115.87, 115.98, 127.17, 135.78, 138.60, 139.07, 154.49, 155.91, 158.41, 164.69. IR (neat,  $\nu$   $\text{cm}^{-1}$ ): 3392, 2928, 1770, 1645, 1615, 905, 970.  $[\text{M}+\text{H}]^+$  calculated for ( $\text{C}_{17}\text{H}_{16}\text{N}_2\text{O}_4$ ) 351.0742 found 351.0737. Melting point: 254  $^\circ\text{C}$

**(Z)-1-((1-(2-(1H-indol-3-yl)ethyl)-5-(hydroxymethyl)-1H-pyrrol-2-yl)methylene)-6-methylfuro[3,4-c]pyridine-3,4(1H,5H)-dione (3d)**

Following the general procedure, the desired compound **3d** was synthesized from (furopyridindione (200mg, 1.21 mmol), 1-(2-(1H-indol-3-yl)ethyl)-5-(hydroxymethyl)-1H-pyrrole-2-carbaldehyde (324mg, 1.21 mmol) and piperidine (0.12 ml, 1.21 mmol). A orange solid was generated with yield of 85%.

$^1\text{H}$  NMR (400 MHz; DMSO- $d_6$ ):  $\delta$  2.70 (s, 3H); 3.09-3.06 (m, 2H); 4.46-4.40 (m, 3H); 5.18-5.16 (t,  $J$  = 5.32 Hz, 1H); 5.97 (s, 1H); 6.22-6.21 (d,  $J$  = 3.88 Hz, 1H); 6.35 (s, 1H); 6.79-6.78 (d,  $J$  = 3.88 Hz, 1H); 6.93 (s, 1H); 7.04-7.01 (m, 1H); 7.10-7.07 (m, 1H); 7.30-7.28 (d,  $J$  = 7.96 Hz, 1H); 7.61-7.59 (d,  $J$  = 7.68 Hz, 1H); 10.79 (s, 1H); 11.83 (s, 1H).  $^{13}\text{C}$  NMR (100 MHz; DMSO- $d_6$ ):  $\delta$  19.65, 19.92, 27.76, 44.35, 55.69, 68.27, 96.52, 99.82, 102.32, 104.46, 109.31, 111.09, 111.29, 111.91, 115.51, 118.65, 118.86, 121.54, 124.19, 127.26, 127.55, 136.68, 138.40, 138.56, 154.08, 155.05, 155.63, 158.36, 164.67, 167.42, 168.73. IR (neat,  $\nu$   $\text{cm}^{-1}$ ): 3310, 2927, 1754, 1733, 1668, 1607, 1141.  $[\text{M}+\text{H}]^+$  calculated for ( $\text{C}_{24}\text{H}_{21}\text{N}_3\text{O}_4$ ) 416.1605 found 416.1596. Melting point: 238  $^\circ\text{C}$

**(Z)-1-((5-(hydroxymethyl)-1-phenethyl-1H-pyrrol-2-yl)methylene)-6-methylfuro[3,4-c]pyridine-3,4(1H,5H)-dione (3e)**

Following the general procedure, the desired compound **3e** was synthesized from (furopyridindione (200mg, 1.21 mmol), 5-(hydroxymethyl)-1-phenethyl-1H-pyrrole-2-carbaldehyde (277mg, 1.21 mmol) and piperidine (0.12 ml, 1.21 mmol). A yellow solid was generated with yield of 82%.

$^1\text{H}$  NMR (400 MHz; DMSO- $d_6$ ):  $\delta$  2.33 (s, 3H); 2.95-2.92 (m, 2H); 4.28-4.27 (d,  $J$  = 5.32 Hz, 2H); 4.43-4.36 (m, 2H); 5.15-5.12 (t,  $J$  = 5.32 Hz, 1H); 6.19-6.18 (d,  $J$  = 3.88 Hz, 1H); 6.78-6.78 (d,  $J$  = 9.00 Hz, 2H); 6.83-6.82 (d,  $J$  = 3.84 Hz, 1H); 7.18-7.14 (m, 3H); 7.26-7.23 (m, 2H); 11.91 (s, 1H).  $^{13}\text{C}$  NMR (100 MHz; DMSO- $d_6$ ):  $\delta$  19.98, 37.96, 44.99, 55.60, 97.03, 102.39, 104.67, 111.25, 115.88, 126.86, 126.96, 128.69, 129.47, 138.54, 138.90, 138.97, 154.24, 155.89, 158.39, 164.69. IR (neat,  $\nu$   $\text{cm}^{-1}$ ): 3457, 2915, 1778, 1755, 1665, 1613, 1258.  $[\text{M}+\text{H}]^+$  calculated for ( $\text{C}_{22}\text{H}_{20}\text{N}_2\text{O}_4$ ) 377.1496 found 377.1484. Melting point: 233  $^\circ\text{C}$

**(Z)-1-((5-(hydroxymethyl)-1-phenyl-1H-pyrrol-2-yl)methylene)-6-methylfuro[3,4-c]pyridine-3,4(1H,5H)-dione (3f)**

Following the general procedure, the desired compound **3f** was synthesized from (furopyridindione (200mg, 1.21 mmol), 5-(hydroxymethyl)-1-phenyl-1H-pyrrole-2-carbaldehyde (243mg, 1.21 mmol) and piperidine (0.12 ml, 1.21 mmol). A brown solid was generated with yield of 81%.

$^1\text{H}$  NMR (400 MHz; DMSO- $d_6$ ):  $\delta$  2.21 (s, 3H); 4.25-4.20 (m, 2H); 5.05 (s, 1H); 6.06 (s, 1H); 6.28 (s, 1H); 6.31 (s, 2H); 6.54-6.44 (d,  $J$  = 3.92 Hz, 1H); 7.05-7.04 (d,  $J$  = 3.88 Hz, 1H); 7.40-7.38 (d,  $J$  = 6.12 Hz, 2H); 7.59-7.56 (m, 2H); 12.11 (s, 1H).  $^{13}\text{C}$  NMR (100 MHz; DMSO- $d_6$ ):  $\delta$  19.65, 55.60, 68.26, 96.38, 99.80, 101.83, 104.87, 109.32, 111.54, 116.32, 128.14, 128.92, 129.33, 129.93, 136.54, 139.54, 139.75, 155.05, 155.29, 158.28, 158.34, 164.52, 167.39, 168.71. IR (neat,  $\nu$   $\text{cm}^{-1}$ ): 3456, 2919, 1757, 1612, 1271.  $[\text{M}+\text{H}]^+$  calculated for ( $\text{C}_{20}\text{H}_{16}\text{N}_2\text{O}_4$ ) 349.1183 found 349.1177. Melting point: 290  $^\circ\text{C}$

**(Z)-1-((1-(4-fluorophenyl)-5-(hydroxymethyl)-1H-pyrrol-2-yl)methylene)-6-methylfuro[3,4-c]pyridine-3,4(1H,5H)-dione (3g)**

Following the general procedure, the desired compound **3g** was synthesized from (furopyridindione (200mg, 1.21 mmol), 1-(4-fluorophenyl)-5-(hydroxymethyl)-1H-pyrrole-2-carbaldehyde (264mg, 1.21 mmol) and piperidine (0.12 ml, 1.21 mmol). A yellow solid was generated with yield of 83%.

<sup>1</sup>H NMR (400 MHz; DMSO-d<sub>6</sub>): δ 2.22 (s, 3H); 4.21-4.19 (d, *J* = 5.28 Hz, 2H); 5.04-5.01 (m, 1H); 6.08 (s, 1H); 6.43-6.41 (m, 2H); 7.03-7.02 (d, *J* = 3.88 Hz, 1H); 7.47-7.39 (m, 4H); 11.93 (s, 1H). <sup>13</sup>C NMR (100 MHz; DMSO-d<sub>6</sub>): δ 19.66, 55.49, 96.61, 101.74, 104.91, 111.60, 116.24, 116.67, 116.89, 128.48, 131.10, 131.19, 132.88, 139.72, 154.98, 155.37, 158.27, 161.09, 163.53, 164.50. IR (neat, ν cm<sup>-1</sup>): 3467, 2919, 1760, 1640, 1614, 1273, 996. [M+H]<sup>+</sup> calculated for (C<sub>20</sub>H<sub>15</sub>FN<sub>2</sub>O<sub>4</sub>) 367.1089 found 367.1080. Melting point: 303 °C

**(Z)-1-((1-(4-chlorophenyl)-5-(hydroxymethyl)-1H-pyrrol-2-yl)methylene)-6-methylfuro[3,4-c]pyridine-3,4(1H,5H)-dione (3h)**

Following the general procedure, the desired compound **3h** was synthesized from (furopyridindione (200mg, 1.21 mmol), 1-(4-chlorophenyl)-5-(hydroxymethyl)-1H-pyrrole-2-carbaldehyde (284mg, 1.21 mmol) and piperidine (0.12 ml, 1.21 mmol). A yellow solid was generated with yield of 87%.

<sup>1</sup>H NMR (400 MHz; DMSO-d<sub>6</sub>): δ 2.23 (s, 3H); 4.21-4.20 (d, *J* = 5.04 Hz, 2H); 5.06-5.03 (m, 1H); 6.13 (s, 1H); 6.46-6.43 (m, 2H); 7.04-7.03 (d, *J* = 3.88 Hz, 1H); 7.44-7.42 (d, *J* = 8.60 Hz, 2H); 7.65-7.62 (d, *J* = 8.60 Hz, 2H); 11.92 (s, 1H). <sup>13</sup>C NMR (100 MHz; DMSO-d<sub>6</sub>): δ 19.68, 55.46, 96.73, 101.72, 104.94, 111.84, 116.42, 128.34, 129.95, 130.75, 133.87, 135.52, 139.56, 139.88, 155.02, 155.40, 158.27, 164.49. IR (neat, ν cm<sup>-1</sup>): 3419, 2920, 1775, 1643, 1615, 1276, 745. [M+H]<sup>+</sup> calculated for (C<sub>20</sub>H<sub>15</sub>ClN<sub>2</sub>O<sub>4</sub>) 383.0793 found 383.0782. Melting point: 285 °C

**(Z)-1-((5-(hydroxymethyl)-1-(4-hydroxyphenyl)-1H-pyrrol-2-yl)methylene)-6-methylfuro[3,4-c]pyridine-3,4(1H,5H)-dione (3i)**

Following the general procedure, the desired compound **3i** was synthesized from (furopyridindione (200mg, 1.21 mmol), 5-(hydroxymethyl)-1-(4-hydroxyphenyl)-1H-pyrrole-2-carbaldehyde (262mg, 1.21mmol) and piperidine (0.12 ml, 1.21 mmol). A brown solid was generated with yield of 82%.

<sup>1</sup>H NMR (400 MHz; DMSO-d<sub>6</sub>): δ 2.22 (s, 3H); 4.19-4.17 (d, *J* = 5.04 Hz, 2H); 4.99 (s, 1H); 5.13 (s, 1H); 6.07 (s, 1H); 6.31 (s, 2H); 6.39-6.38 (d, *J* = 3.88 Hz, 1H); 6.92-6.89 (d, *J* = 8.60 Hz, 1H); 7.01-7.00 (d, *J* = 3.88 Hz, 1H); 7.17-7.15 (d, *J* = 8.60 Hz, 2H); 9.89 (s, 1H). <sup>13</sup>C NMR (100 MHz; DMSO-d<sub>6</sub>): δ 19.61, 19.65, 55.66, 68.25, 96.35, 99.80, 102.10, 104.77, 109.32, 111.13, 116.07, 116.33, 127.48, 128.36, 130.00, 139.27, 140.11, 154.97, 155.04, 155.26, 158.07, 158.34, 164.56, 167.40, 168.70. IR (neat, ν

cm<sup>-1</sup>): 3429, 2927, 1754, 1612, 1273, 1237. [M+H]<sup>+</sup> calculated for (C<sub>20</sub>H<sub>16</sub>N<sub>2</sub>O<sub>5</sub>) 365.1132 found 365.1117. Melting point: 278 °C

**(Z)-1-((5-(hydroxymethyl)-1-(o-tolyl)-1H-pyrrol-2-yl)methylene)-6-methylfuro[3,4-c]pyridine-3,4(1H,5H)-dione (3j)**

Following the general procedure, the desired compound **3j** was synthesized from (furopyridindione (200mg, 1.21 mmol), 5-(hydroxymethyl)-1-(o-tolyl)-1H-pyrrole-2-carbaldehyde (260mg, 1.21 mmol) and piperidine (0.12 ml, 1.21 mmol). A orange solid was generated with yield of 84%.

<sup>1</sup>H NMR (400 MHz; DMSO-d<sub>6</sub>): δ 1.88 (s, 3H); 2.20 (s, 3H); 4.10-4.09 (m, 2H); 4.94 (s, 1H); 5.81 (s, 1H); 6.21 (s, 1H); 6.46-6.45 (d, *J* = 3.84 Hz, 1H); 7.05-7.04 (d, *J* = 3.84 Hz, 1H); 7.30-7.28 (d, *J* = 7.52 Hz, 1H); 7.42-7.39 (m, 1H); 7.50-7.45 (m, 2H); 11.90 (s, 1H). <sup>13</sup>C NMR (100 MHz; DMSO-d<sub>6</sub>): δ 17.18, 19.62, 55.57, 96.29, 101.21, 104.89, 111.38, 116.12, 127.45, 127.77, 129.59, 130.00, 131.37, 135.60, 137.16, 139.30, 139.55, 155.05, 155.20, 158.26, 164.46. IR (neat, ν cm<sup>-1</sup>): 3420, 2920, 1751, 1636, 1607, 1347, 1264. [M+H]<sup>+</sup> calculated for (C<sub>21</sub>H<sub>18</sub>N<sub>2</sub>O<sub>4</sub>) 363.1339 found 363.1336. Melting point: 289 °C

**(Z)-ethyl 4-(2-(hydroxymethyl)-5-((6-methyl-3,4-dioxo-4,5-dihydrofuro[3,4-c]pyridin-1(3H)-ylidene)methyl)-1H-pyrrol-1-yl)benzoate (3k)**

Following the general procedure, the desired compound **3k** was synthesized from (furopyridindione (200mg, 1.21 mmol)), ethyl 4-(2-formyl-5-(hydroxymethyl)-1H-pyrrol-1-yl)benzoate (330mg, 1.21 mmol) and piperidine (0.12 ml, 1.21 mmol). A yellow solid was generated with yield of 87%.

<sup>1</sup>H NMR (400 MHz; DMSO-d<sub>6</sub>): δ 1.37-1.34 (t, *J* = 7.08 Hz, 3H); 2.21 (s, 3H); 4.24-4.22 (s, *J* = 5.28 Hz, 2H); 4.40-4.35 (q, *J*<sub>1</sub> = 7.12 Hz and *J*<sub>2</sub> = 7.08 Hz, 2H); 5.09-5.06 (m, 1H); 6.15 (s, 1H); 6.47-6.45 (m, 2H); 7.07-7.06 (d, *J* = 3.88 Hz, 1H); 7.57-7.54 (d, *J* = 8.52 Hz, 2H); 8.15-8.13 (m, 2H); 11.96 (1.09). <sup>13</sup>C NMR (100 MHz; DMSO-d<sub>6</sub>): δ 14.64, 19.67, 55.47, 61.52, 96.75, 101.65, 104.96, 112.09, 116.63, 128.18, 129.24, 130.39, 130.80, 139.42, 139.97, 140.78, 155.03, 155.42, 158.25, 165.63. IR (neat, ν cm<sup>-1</sup>): 3400, 2926, 1748, 1713, 1639, 1614, 1274, 1239. [M+H]<sup>+</sup> calculated for (C<sub>23</sub>H<sub>20</sub>N<sub>2</sub>O<sub>6</sub>) 421.1394 found 421.1380. Melting point: 284 °C

*Enzymatic assays.* The inhibitory effect of the synthesized compounds on α-glucosidase (yeast origin),

α-fucosidase (bovine kidney origin) and α-mannosidase (jack bean origin) inhibitory activity was determined in 96-well plates employing the substrate PNPG and 4-nitrophenyl α-D-glucopyranoside according to the procedure previously reported by Ferreres *et al.*<sup>42</sup> Prior to use, all test compounds were solubilised in solvent, dimethylsulfoxide (DMSO), and then further diluted in DMSO to acquire the desired final maximum test concentration. Briefly, each well in 96-well plates contained 100 μL

of 2 mM 4-nitrophenyl  $\alpha$ -D-glucopyranoside (PNP-G) in 10 mM potassium phosphate buffer (pH 7.2) and different test concentrations (2–10  $\mu$ M). The reaction was initiated by the addition of 5  $\mu$ L of the enzyme solution (0.1 IU per well).  $\alpha$ -glucosidase (yeast),  $\alpha$ -fucosidase (bovine kidney) and  $\alpha$ -mannosidase (jack bean) were purchased from Sigma Aldrich, Bangaluru). The plates were incubated at 37 °C for 10 min. The absorbance was measured spectrophotometrically at 430 nm (Spectra Max M5e micro plate reader). The increase in absorbance ( $\Delta A$ ) was compared with that of the control (buffer instead of test compound) to compute the inhibitory concentrations (IC<sub>50</sub>) which was determined from three independent assays replicated thrice. Acarbose, an illustrious inhibitor of  $\alpha$ -glucosidase was employed as positive control. Inhibition (%) =  $(\Delta A_{\text{control}} - \Delta A_{\text{sample}}/\Delta A_{\text{control}} \times 100)$ . The concentration of compound required to obtain 50% inhibition of  $\alpha$ -glycosidase activity under the assay conditions was defined as the IC<sub>50</sub> value. Data are average of three independent sets of assays performed replicated thrice

**Reaction kinetics:** The inhibition kinetics against  $\alpha$ -glucosidase was determined by adding increasing concentrations of pNPG (1, 2, 3, 4 and 5 mM respectively) as substrate, in the absence and presence of compound 3k as inhibitor at 2 and 10  $\mu$ M for yeast enzyme. The absorbance was measured spectrophotometrically at 420 nm (Biorad micro elisa plate reader (iMark)). The mode of inhibition (i.e. competitive, non-competitive, uncompetitive or mixed type) of the screened compounds was determined on the basis of the inhibitory effects on  $K_m$  (Michaelis constant) and  $V_{\text{max}}$  (maximum reaction velocity) of the enzyme. The study was computed using the primary (Lineweaver–Burk) plots, which are the double reciprocal plots of enzyme reaction velocities ( $1/V$ ) versus substrate concentrations ( $1/[S]$ ). The Lineweaver–Burk (LB) equation follows as:

$$V = \frac{V_{\text{max}}[S]}{K_m + [S]}$$

where,  $V$  is the reaction velocity;  $K_m$  is Michaelis-Menten constant;  $V_{\text{max}}$  is the maximum velocity and  $[S]$  is the substrate concentration.

**Intrinsic fluorescence measurements:**  $\alpha$ -Glucosidase (1.5U) was pre-treated with certain concentrations of compound 3k (6.25 and 25 ng/ml respectively) for 30 min at 37°C. The intrinsic fluorescence spectra (300-440 nm) were measured using HORIBA Fluorolog-3 spectrofluorometer (Model: FL3-2-IHR) with the excitation wavelength at 260 nm.

**Circular dichroism:** Circular dichroism (CD) was carried out with a J-1500 spectrometer (Jasco) in the UV range (195-240 nm) using 0.1 cm quartz cuvette. Different concentration of compound 11 was added to  $\alpha$ -glucosidase (30 U/ml). The CD spectra were recorded with 3 times accumulation. The

data of the secondary structure were dealt with by using the professional software Secondary Structure Estimation.

**Modelling of alpha-glucosidase structure:** Three-dimensional (3D) structure of the alpha-glucosidase (MAL32\_YEAST) protein sequence from *Saccharomyces cerevisiae* was modelled using isomaltase from *Saccharomyces cerevisiae* (PDB ID: 3AJ7) as a template which possesses 72% sequence identity with the alpha-glucosidase (MAL32). MODELLER v9.16 was used to build the structure and top ten models were filtered based on the DOPE score.<sup>43</sup> The filtered models were subjected to Procheck, Verify3D, and Errat programs in order to check stereo-chemical properties and fold compatibility of the predicted models.<sup>44-46</sup> Based on these parameters, the most likely 3D model of *S. cerevisiae* alpha-glucosidase (MAL32) was selected for further analysis.

**Molecular Docking:** The predicted alpha-glucosidase structure was subjected to CASTp server in order to identify the probable binding pocket and the largest pocket was selected to dock the compound **3k**.<sup>47</sup> The docking analysis was performed using GOLD docking tool and docking poses were ranked using CHEMPLP scoring function.<sup>48</sup>  $\Delta G$  of binding was calculated using the MOPAC2016 program.<sup>49</sup> The protein-ligand interaction analysis was performed using the Ligplot program to identify interacting residues.<sup>50</sup>

**Thermodynamic solubility:** Solubility of the compound was determined by incubating 1mg of compound in 1 mL of phosphate buffer saline for 24h with the vortex of 500 rpm. After incubation period, samples were centrifuged and supernatant was injected into HPLC to determine the solubility.

**Log D determination:** The distribution coefficient was determined by adding compound 3k to Octanol containing 2 mL deep well plate and vortexed the plate for 10 Min at 1200 g and then 500 $\mu$ L of Buffer was added to it. This plate was incubated at room temperature for 1 hr on a plate shaker at 1200 g. After incubation, the samples were allowed to equilibrate for 20 min and then samples were centrifuged at 4000 g for 30 min. Octanol and buffer layers were analyzed by HPLC-UV by adjusting the needle height for each Octanol and buffer.

**PAMPA permeability:** PAMPA permeability was determined by addition of the compound 3k to the donor (bottom) plate of the PAMPA sandwich plate and 5  $\mu$ L of the GIT-0 solution was painted at the bottom side of the PAMPA acceptor plate by turning the plate upside down. The painted acceptor plate was placed on top of the donor plate in its normal position. The acceptor sink buffer was added to the acceptor plate. The PAMPA sandwich plate was kept for incubation for 4 hours. After 4 hours incubation, 150  $\mu$ L was aliquots from donor and acceptor plate were added to UV analysis plate and read by PAMPA explorer software.

**Metabolic stability in mouse, rat and human liver microsomes:** Metabolic stability is defined as the percentage of parent compound lost over time in the presence of a metabolically active test system. The incubation mixtures consisted of liver microsomes (1.0 mg microsomal protein/mL), compound **3k** (1  $\mu$ M) or positive control (verapamil, 1  $\mu$ M). The reactions were initiated by adding 1 mM NADPH. Reactions without NADPH (0 and 60 min) were also incubated to rule out non-NADPH metabolism or chemical instability in the incubation buffer. All reactions were terminated using 200  $\mu$ L of ice-cold acetonitrile containing internal standard (200 ng/mL of telmisartan) at 0, 5, 15, 30 and 60 min. The vials were centrifuged at 4000 rpm for 20 min. The supernatants thus obtained were analyzed on LC-MS/MS to monitor the disappearance of compound **3k**.

**Plasma protein binding in mouse, rat and human plasma:** To evaluate the ability of compound **3k** to bind the plasma proteins, the most common approach of plasma protein binding using rapid equilibrium dialysis device (RED inserts) used. Compound **3k** was tested at a final concentration of 10  $\mu$ M in mouse, rat and dog plasma. An aliquot of 500  $\mu$ L plasma containing compound **3k** was added in first half (plasma side) of the well of RED device. An aliquot of 300  $\mu$ L of 100 mM sodium phosphate buffer pH 7.4 was added in the second half (buffer side) of the Insert. The plate containing plasma and buffer was equilibrated at  $37 \pm 1$  °C for 6h, with constant shaking at 500 rpm on an orbital shaker. Samples were collected from respective halves after the completion of the incubation time. The proteins were precipitated using organic solvents. The samples were subjected to centrifugation and the supernatants were analyzed analysis on LC-MS/MS

**Pharmacokinetics in mice:** Swiss albino mice were obtained from Hylasco, Hyderabad, India. They were housed under standard conditions and were maintained under a 12 h light/dark cycle in the laboratory animal resources facilities, Acubiosys Pvt. Ltd, Hyderabad, India (AAALAC accredited). Mice were fasted overnight before and then until 3 h after dosing. Water was allowed ad libitum during the fasting period. The bodyweights of individual mice, ranging from 25 to 30 g, were determined on the morning of the study. Compound **3k** was administered orally to twelve mice at 3mg/kg. Since this is the preliminary pharmacokinetic study, the dosage was based on the initial solubility studies of **3k**. After dosing, 0.1 ml specimens of blood were collected by stagger sampling with two bleeds per mouse from the retro orbital plexus at 0.25, 0.5, 1, 2, 4, 8, and 24 h after PO route. After collection, blood was processed to plasma by centrifugation at 10000 rpm for 5 min, and samples were analysed by LC-MS/MS.

**In vivo efficacy in rats:** Male Sprague-Dawley rats (250 - 320 g) approximately 8 -10 weeks old were purchased from the Hylasco Laboratories Hyderabad for the experiments. All the experiments were

performed in accordance with the committee for the purpose of Control and Supervision of Experiments on Animals (CPCSEA) guidelines. For each treated group six animals were used. Diabetic rats were administered a single dose of streptozotocin (STZ, 70 mg/kg, Intraperitoneal) formulated in 0.1 mmol/L citrate buffer, pH 4.5 (Sigma–Aldrich, India). 4 days after the STZ injection, the random blood glucose level of the diabetic rats was measured to confirm hyperglycaemia. Random blood glucose above 125 mg/dl was used to define rats as diabetic. Above blood glucose level were compared with normal vehicle control animals (n=6). Diabetic rats were fed a Normal diet throughout the experiment. Diabetic rats with a similar degree of hyperglycaemia were randomly divided into three groups: Diabetic vehicle, Diabetic acarbose, and compound **3k** groups (n=6, in each group).

The typical human daily dose of acarbose is 300 mg/60 kg body weight. According to the formula:  $d_{\text{rat}} = d_{\text{human}} \times 0.71/0.11$ , the corresponding dose of acarbose for rats is 32.28 mg/kg per day. 60 mg/kg per day as high dosages. The control (n=6) and the diabetic group received 0.5% saline, whereas the Acarbose (TCI Chemical, Chennai, India) and compound **3k** groups were given doses of 60 and 60 mg/kg in a 0.5% saline solution respectively. The drug was administered once daily for 4 weeks using a gastric gavage. All animals were housed in an environmentally controlled room at 25°C with a 12 h light-dark cycles and were given free access to food and water throughout the experimental period. Fasting animals were allowed free access to water. After 4 weeks of treatment, blood samples were taken from rats after anaesthesia. The rats were then sacrificed. All procedures involving animals were approved by the IAEC (institutional animal ethics committee).

Statistical analysis results are expressed as the mean  $\pm$  standard deviation. Statistical analysis was performed with 2-way ANOVA.  $P < 0.0001$  was considered statistically significant. Analysis performed with Graph prism 6.01.

Elevated fasting blood glucose levels were measured after 72h of STZ administration. 50% Carbohydrate (w/w), 2% fat (w/w), 18% Protein, 8% fiber and water ad libitum. The fasting time was 6h. Whole blood collected by tail puncture method was checked for blood glucose using Accu-Chek Active meter (Model GB). Volume of blood sample was 1-2 mL. Route of sampling was tail vein puncture. The code or number of protocol approval by the Institutional Animal Ethic BITS/IAEC/2018/13.

Please refer below for the glycaemic value of the control groups in the table below.

**Table 6.** The glycaemic values of the control groups

S. No.	Group	B.Wt on 25/01/2019	25/01/2019 Dose Volume	Fasting Glucose (mg/dl)
1	Control	300.30	1.5 ml	95
2		295.21	1.5 ml	89
3		278.12	1.4 ml	90
4		281.21	1.4 ml	91
5		301.21	1.5 ml	90
6		294.14	1.5 mL	94

**MTT assay for beta cell proliferation:** BRIN-BD11 cells (rat beta cell line) were seeded in a 96-well plate at a density of  $10^4$  cells/well in 100 $\mu$ l of RPMI complete medium and were incubated overnight. Cells were then exposed to different concentrations of compound (100 $\mu$ M, 30 $\mu$ M, 10 $\mu$ M, 3 $\mu$ M, 1 $\mu$ M, 0.3 $\mu$ M, 0.1 $\mu$ M) in 100 $\mu$ l medium. After 24 h, 10 $\mu$ l of MTT reagent (5mg/ml) was added to each well and cells were incubated at 37 $^{\circ}$ C for 90 mins to allow the formation of formazan crystals (MTT is reduced to formazan). Post incubation, medium was replaced with 100 $\mu$ l of DMSO to dissolve formazan crystals and absorbance at 560nm was measured using flat a microplate reader.

#### ACKNOWLEDGEMENT

We thank Shiv Nadar University for financial support. We thank BITS Pilani, Hyderabad to allow us to use the J-1500 spectrometer (Jasco) to execute Circular dichroism (CD).

#### ASSOCIATED CONTENT

##### Supporting information available

Details of synthetic procedures for compounds **3a** - **3k** and  $^1\text{H}$  and  $^{13}\text{C}$  NMR spectra. This material is available free of charge via the Internet at <http://pubs.acs.org>. The CCDC# for the X-Ray structure of compound **3k** is 1934521. Authors will release the coordinates of the homology model upon article publication.

#### AUTHOR INFORMATION

##### Corresponding Author

\*Phone : +919810250221. Email: [subhabrata.sen@snu.edu.in](mailto:subhabrata.sen@snu.edu.in)

##### Notes

The authors declare no competing financial interest

#### ABBREVIATIONS USED

STZ, streptozotocin; DM, diabetes mellitus; T1DM, type 1 diabetes mellitus; T2DM, type 2 diabetes mellitus; PBG, post-prandial blood glucose; AGI,  $\alpha$ -glucosidase inhibitors; PPAR- $\gamma$ , peroxime proliferator-activated receptor; DAB, 4-dideoxy-1, 4-imino-D<sub>2</sub>-arabonitol; PNPG, *p*-nitrophenyl- $\beta$ -D-glucopyranoside; Trp, tryptophan; CD, circular dichroism; DMPK, drug metabolism and pharmacokinetics; ADME, adsorption, metabolism and excretion; DDI, drug-drug interaction.

## References

1. K. Ogurtsova, J.D. da Rocha Fernandes, Y. Huang, U. Linnenkamp, L. Guariguata, N.H. Cho, D. Cavan, J.E. Shaw, L.E. Makaroff, IDF Diabetes Atlas: Global estimates for the prevalence of diabetes for 2015 and 2040, *Diabetes Res. Clin. Pract.* 128 (2017) 40–50.
2. N. Al-Hassan, Definition of diabetes mellitus, *Br. J. Gen. Pract.* 53 (2003) 567–568.
3. W.T. Cade, Diabetes-related microvascular and macrovascular diseases in the physical therapy setting, *Phys. Ther.* 88 (2008) 1322-1335.
4. D. Care, 2. Classification and diagnosis of diabetes, *Diabetes Care* 38 (2015) 8-16.
5. S. Ogawa, K. Nako, M. Okamura, T. Sakamoto, S. Ito, Stabilization of postprandial blood glucose fluctuations by addition of glucagon like polypeptide-analog administration to intensive insulin therapy, *J. Diabetes Investig.* 6 (2015) 436-442.
6. (a) U. Ghani, Re-exploring promising  $\alpha$ -glucosidase inhibitors for potential development into oral anti-diabetic drugs: Finding needle in the haystack, *Eur. J. Med. Chem.* 103 (2015) 133-162. (b) K. Wang, L. Bao, K. Ma, J. Zhang, B. Chen, J. Han, J. Ren, H. Luo, H. Liu, A novel class of  $\alpha$ -glucosidase and HMG-CoA reductase inhibitors from *Ganoderma leucocontextum* and the anti-diabetic properties of ganomycin 1 in KK-A<sup>y</sup> mice, *Eur. J. Med. Chem.* 127 (2017) 1035-1045. (c) K. Wang, L. Bao, N. Zhou, J. Zhang, M. Liao, Z. Zheng, Y. Wang, C. Liu, L. Wang, W. Wang, S.J. Liu, H. Liu, Structural modification of natural product ganomycin 1 leading to discovery of a  $\alpha$ -glucosidase and HMG-CoA reductase dual inhibitor improving obesity and metabolic dysfunction in vivo, *J. Med. Chem.* 61 (2018) 3609-3625. (d) S. Rocha, D. Rebeiro, E. Fernandes, M. Freitas, Systematic review on anti-diabetic properties of chalcones, *Curr. Med. Chem.* 25 (2018) DOI: 10.2174/0929867325666181001112226
7. D. Dicker, DPP-4 inhibitors: impact on glycemic control and cardiovascular risk factors, *Diabetes Care* 34 (2011) S276-S278.
8. M.J. Davies, Insulin secretagogues, *Curr. Med. Res. Opin.* 18 (2002) s22-s30.
9. L. Michalik, J. Auwerx, J.P. Berger, V.K. Chatterjee, C.K. Glass, F.J. Gonzalez, P.A. Grimaldi, T. Kadowaki, M.A. Lazar, S. O’Rahilly, C.N. Palmer, J. Plutzky, J.K. Reddy, B.M. Spiegelman, B.

- Staels, W. Wahli, International Union of Pharmacology. LXI. Peroxisome proliferator-activated receptors, *Pharmacol. Rev.* 58 (2006) 726-741.
10. M. Tiittanen, J.T. Huupponen, M. Knip, O. Vaarala, Insulin treatment in patients with type 1 diabetes induces upregulation of regulatory T-cell markers in peripheral blood mononuclear cells stimulated with insulin in vitro, *Diabetes* 55 (2006) 3446-3454.
  11. K. Jayarag, E.D. Davis, D. McNeill, New therapies for type 1 diabetes mellitus, *Ochsner J.* 3 (2001) 138-143.
  12. M. DeGeeter, B. Williamson, Alternative agents in type 1 diabetes in addition to insulin therapy: metformin, alpha-glucosidase inhibitors, pioglitazone, GLP-1 agonists, DPP-IV inhibitors, and SGLT-2 inhibitors, *J. Pharm. Pract.* 2 (2016) 144-159.
  13. N. Asano, M. Nishida, M. Miyauchi, K. Ikeda, M. Yamamoto, H. Kizu, Y. Kameda, A.A. Watson, R.J. Nash, G.W. Fleet, Polyhydroxylated pyrrolidine and piperidine alkaloids from *Adenophora triphylla* var. *japonica* (Campanulaceae), *Phytochemistry* 53 (2000) 379-382.
  14. G.C. Kite, L.E. Fellows, G.W. Fleet, P.S. Liu, A.M. Scofield, N.G. Smith,  $\alpha$ -Homonojirimycin [2, 6-dideoxy-2, 6-imino-D-glycero-L-gulo-heptitol] from *omphalea diandra* L.: isolation and glucosidase inhibition. *Tetrahedron Lett.* 29 (1988) 6483-6485.
  15. R.J. Nash, P.I. Thomas, R.D. Waigh, G.W. Fleet, M.R. Wormald, P.M.D.Q. Lilley, D.J. Watkin, Casuarine: a very highly oxygenated pyrrolizidine alkaloid, *Tetrahedron Lett.* 35 (1994) 7849-7852.
  16. M. Yoshikawa, T. Murakami, K. Yashiro, H. Matsuda, Kotalanol, a potent  $\alpha$ -glucosidase inhibitor with thiosugar sulfonium sulfate structure, from antidiabetic Ayurvedic medicine *Salacia reticulata*, *Chem. Pharma. Bull.* 46 (1998) 1339-1340.
  17. H.W. Ryu, B.W. Lee, M.J. Curtis-Long, S. Jung, Y.B. Ryu, W.S. Lee, K.H. Park, Polyphenols from *Broussonetia papyrifera* displaying potent  $\alpha$ -glucosidase inhibition, *J. Agric. Food Chem.* 58 (2010) 202-208.
  18. K. Tadera, Y. Minami, K. Takamatsu, T. Matsuoka, Inhibition of  $\alpha$ -glucosidase and  $\alpha$ -amylase by flavonoids, *J. Nutr. Sci. Vitaminol.* 5 (2006) 149-153.
  19. E.J. Seo, M.J. Curtis-Long, B.W. Lee, H.Y. Kim, Y.B. Ryu, T.S. Jeong, W.S. Lee, K.H. Park, Xanthenes from *Cudrania tricuspidata* displaying potent  $\alpha$ -glucosidase inhibition, *Bioorg. Med. Chem. Lett.* 17 (2007) 6421-6424.
  20. M. Shibano, D. Tsukamoto, A. Masuda, Y. Tanaka, G. Kusano, Two new pyrrolidine alkaloids, radicamines A and B, as inhibitors of  $\alpha$ -glucosidase from *Lobelia chinensis* LOUR, *Chem. Pharm. Bull.* 49 (2001) 1362-1365.

21. D. Yang, J. Zhao, S. Liu, F. Song, Z. Liu, the screening of potential  $\alpha$ -glucosidase inhibitors from the *Polygonum multiflorum* extract using ultrafiltration combined with liquid chromatography-tandem mass spectrometry, *Anal. Methods*. 6 (2014) 3353-3359.
22. M. Liu, W. Zhang, J. Wei, X. Lin, Synthesis and  $\alpha$ -glucosidase inhibitory mechanisms of bis (2, 3-dibromo-4, 5-dihydroxybenzyl) ether, a potential marine bromophenol  $\alpha$ -glucosidase inhibitor, *Mar. Drugs* 9 (2011) 1554-1565.
23. S.H. Lam, J.M. Chen, C.J. Kang, C.H. Chen, S.S. Lee,  $\alpha$ -Glucosidase inhibitors from the seeds of *Syagrus romanzoffiana*, *Phytochemistry* 69 (2008) 1173-1178.
24. J. Sichaem, K. Ingkaninan, S. Tip-pyang, A novel pyrrole alkaloid from the fruit peels of *Strychnos nux-blanda*, *Nat. Prod. Res.* 31 (2017) 149-154.
25. Z.Q. Liu, T. Liu, C. Chen, M.Y. Li, Z.Y. Wang, R.S. Chen, G.X. Wei, X.Y. Wang, D.Q. Luo, Fumosorinone, a novel PTP1B inhibitor, activates insulin signaling in insulin-resistance HepG2 cells and shows anti-diabetic effect in diabetic KKAY mice, *Toxicol. Appl. Pharmacol.* 285 (2015) 61-70.
26. F. Brindis, R. Rodríguez, R. Bye, M. González-Andrade, R. Mata, (Z)-3-butylidenephthalide from *Ligusticum porteri*, an  $\alpha$ -glucosidase inhibitor, *Nat. Prod. Rep.* 74 (2011) 314-320.
27. W.D. Seo, J.H. Kim, J.E. Kang, H.W. Ryu, M.J. Curtis-Long, H.S. Lee, M.S. Yang, K.H. Park, Sulfonamide chalcone as a new class of  $\alpha$ -glucosidase inhibitors, *Bioorg. Med. Chem. Lett.* 15 (2005) 5514-5516.
28. M. Taha, N.H. Ismail, S. Lalani, M.Q. Fatmi, S. Siddiqui, K.M. Khan, S. Imran, M.I. Choudhary, Synthesis of novel inhibitors of  $\alpha$ -glucosidase based on the benzothiazole skeleton containing benzohydrazide moiety and their molecular docking studies, *Eur. J. Med. Chem.* 92 (2005) 387-400.
29. I. Ali, A. Khan, A. Hussain, U. Farooq, M. Ismail, V. Hyder, V.U. Ahmad, V.O. Iaroshenko, H. Hussain, P. Langer, Comparative enzyme inhibition study of 1-deazapurines, *Med. Chem. Res.* 25 (2016) 2599-2606.
30. M. Khan, M. Yousaf, A. Wadood, M. Junaid, M. Ashraf, U. Alam, M. Ali, M. Arshad, Z. Hussain, K.M. Khan, Discovery of novel oxindole derivatives as potent  $\alpha$ -glucosidase inhibitors, *Bioorg. Med. Chem.* 22 (2014) 3441-3448.
31. N.D. Adhikary, S. Kwon, W.J. Chung, S. Koo, One-pot conversion of carbohydrates into pyrrole-2-carbaldehydes as sustainable platform chemicals, *J. Org. Chem.* 80 (2015) 1-26.
32. A. Ghisaidoobe, S. Chung, Intrinsic tryptophan fluorescence in the detection and analysis of proteins: a focus on Förster resonance energy transfer techniques, *Int. J. Mol. Sci.* 15, (2014) 22518-22538.

33. M. Liu, W. Zhang, J. Wei, X. Lin, Synthesis and  $\alpha$ -glucosidase inhibitory mechanisms of bis (2, 3-dibromo-4, 5-dihydroxybenzyl) ether, a potential marine bromophenol  $\alpha$ -glucosidase inhibitor, *Mar. Drugs*. 9 (2011) 1554-1565.
34. L. Zeng, G. Zhang, Y. Liao, D. Gong, Inhibitory mechanism of morin on  $\alpha$ -glucosidase and its anti-glycation properties, *Food Funct*. 7 (2016) 3953-3963.
35. B. Svensson, Protein engineering in the  $\alpha$ -amylase family: catalytic mechanism, substrate specificity, and stability, *Plant Mol. Biol.* 25 (1994) 141-157.
36. Y. Matsuura, M. Kusunoki, W. Harada, M. Kakudo, Structure and possible catalytic residues of Taka-amylase A, *J. Biochem.* 95 (1998) 697-702.
37. R. Nakajima, T. Imanaka, S. Aiba, Comparison of amino acid sequences of eleven different  $\alpha$ -amylases, *Appl. Microbiol. Biotechnol.* 23 (1986) 355-360.
38. B. Svensson, Regional distant sequence homology between amylases,  $\alpha$ -glucosidases, and transglucanoylases, *FEBS Lett.* 230 (1988) 72-76.
39. H. Kubinyi, Drug Research: Myth, hype and reality, *Nat. Rev. Drug Discov.* 2 (2003) 665-668.
40. J.A. Bluestone, K. Herold, G. Eisenbarth, Genetics, pathogenesis and clinical interventions in type 1 diabetes, *Nature* 464 (2010) 1293-1300.
41. A. Lehuen, J. Diana, P. Zaccane, A. Cooke, Immune cell crosstalk in type 1 diabetes, *Nat. Rev. Immunol.* 10 (2010) 501-513.
42. F. Ferreres, J. Vinholes, A. Gil-Izquierdo, P. Valentão, R.F. Gonçalves, P.B. Andrade, In vitro studies of  $\alpha$ -glucosidase inhibitors and antiradical constituents of *Glandora diffusa* (Lag.) DC Thomas infusion, *Food Chem.* 136 (2013) 1390-1398.
43. A. Šali, T.L. Blundell, Comparative protein modelling by satisfaction of spatial restraints, *J. Mol. Biol.* 234 (1993) 779-815.
44. R.A. Laskowski, M.W. MacArthur, D.S. Moss, J.M. Thornton, PROCHECK: a program to check the stereochemical quality of protein structures, *J. App. Cryst.* 26 (1993) 283-291.
45. R. Lüthy, J.U. Bowie, D. Eisenberg, Assessment of protein models with three-dimensional profiles, *Nature* 356 (1992) 83-85.
46. S.C. Lovell, I.W. Davis, W.B. Arendall III, P.I. De Bakker, J.M. Word, M.G. Prisant, J.S. Richardson, D.C. Richardson, Structure validation by  $C\alpha$  geometry:  $\varphi$ ,  $\psi$  and  $C\beta$  deviation, *Proteins: Structure, Function, and Bioinformatics* 50 (2003) 437-450.
47. W. Tian, C. Chen, X. Lei, J. Zhao, J. Liang, CASTp 3.0: computed atlas of surface topography of proteins, *Nucleic Acids Res.* 46 (2018) W363-W367.
48. G. Jones, P. Willett, R.C. Glen, A.R. Leach, R. Taylor, Development and validation of a genetic algorithm for flexible docking, *J. Mol. Biol.*, 267 (1997) 727-748.

49. MOPAC2016, James J. P. Stewart, Stewart Computational Chemistry, Colorado Springs, CO, USA, [HTTP://OpenMOPAC.net](http://OpenMOPAC.net) (2016).
50. A.C. Wallace, R.A. Laskowski, J.M. Thornton, LIGPLOT: a program to generate schematic diagrams of protein-ligand interactions. *Protein engineering, design and selection* 8 (1995) 127-134.

Journal Pre-proof

**Highlights**

1. Pyrido-pyrrolidine hybrids were designed as  $\alpha$ -glucosidase inhibitors.
2. The design is based on screening of fragments of reported  $\alpha$ -glucosidase inhibitors and antidiabetic compounds.
3. The most active fragments were stitched to provide the pyrido-pyrrolidine hybrids
4. Compounds were synthesized through Knoevenagel reaction
5. Screening against  $\alpha$ -glucosidase resulted in **3k** as most efficacious with  $IC_{50}$  of 0.56  $\mu$ M.
6. Photoluminescence and circular dichroism study indicated that **3k** binds to the 1° and 2° structure of the enzyme.
7. *In vivo* experiment show that **3k**, remits the fasting blood glucose level for T1 diabetic male Sprague-Dawley rats (250–320 g)
8. At lower concentration, compound **3k** slightly stimulates proliferation of BRIN-BD11 cells.

**Declaration of interests**

The authors declare that they have no known competing financial interests or personal relationships that could have appeared to influence the work reported in this paper.

The authors declare the following financial interests/personal relationships which may be considered as potential competing interests:



Dr. Subhabrata Sen  
Professor,  
Department of Chemistry  
School of Natural Sciences  
Shiv Nadar University, UP 201314, India